THE SIMULATION OF POWER - FREQUENCY TRANSIENTS

A Thesis Submitted
in Partial Fulfilment of the Requirements
for the Degree of
MASTER OF TECHNOLOGY

By
VINNAKOTA BAPI RAJU

to the
DEPARTMENT OF ELECTRICAL ENGINEERING
INDIAN INSTITUTE OF TECHNOLOGY, KANPUR
DECEMBER, 1978

CERTIFICATE

It is certified that the work entitled "Simulation of Power-Frequency Transients" by Mr. Vinnakota Bapi Raju has been carried out under my supervision and has not been submitted elsewhere for the award of degree.

December 1978.

R.P. Aggarwal
Professor
Department of Electrical Engineering
Indian Institute of Technology
Kanpur

ACKNOWLEDGEMENTS

I take this opportunity to express my indebtedness and deep sense of gratitude to Dr. R.P. Aggarwal who initiated me to this problem and provided excellent guidance throughout the course of this work.

I express my indebtedness to Dr. K.R.Padiyar for many useful discussions and suggestions.

I wish to acknowledge my indebtedness to my teachers C. Radhakrishna and Dr. C. Laxminarayana for their interest shown during the progress of this thesis.

I am grateful to Ers. A.K. Mitra, A.K. Rastogi, V.P. Tiwari and S.K. Garg for providing the UPSEB system data and for useful discussions.

Thanks are due to fellow research scholars K.S. Sarma, R.P.Adgaonkar, Mrs. K.Gomathi, N. Arumugam, R.P.Suri, V.V. Rao and T.V. Prabhakar for useful discussions.

The help rendered by my friends P.D. Porey and Kultar Singh is appreciated. I would like to thank Mr. K.N. Tewari for the care and interest taken in typing the manuscript.

Vinnakota Bapi Raju

TABLE OF CONTENTS

		Page
LIST OF FIGURES		
LIST OF TABLES		
NOMENCLATURE		
ABSTRACT		
CHAPTER 1 :	INTRODUCTION	1
1.1	General discussion	1
1.2	Previous work	3
1.3	Details of problem under consideration	6
CHAPTER 2 :	TURBINE AND SPEED GOVERNOR MODELS	9
2.1	General discussion	9
2.2	Speed governor and thermal turbine model	9
2.3	Speed governor and hydro turbine model	14
CHAPTER 3 :	IMPLEMENTATION TREATING ELECTRICAL LOADING CONSTANT	19
3.1	General discussion	19
3.2	Implementation	20
3.3	Discussion and Conclusions	24
CHAPTER 4 :	GENERATOR AND EXCITATION SYSTEM MODELS	29
4.1	Generator representation	29
4.2	Excitation system model	31
CHAPTER 5 :	IMPLEMENTATION INCLUDING ELECTRICAL LOADING	37
5.1	General Discussion	37
5.2	Calculation of total electrical power output P_{eT}	38

5.3 Digital simulation 42

5.4 Step by Step algorithm for implementation on digital computer 42

5.5 Computer results for IEEE-14 bus system 45

5.6 Computer results for UPSEB planning model network 47

CHAPTER 6 : OVERALL CONCLUSIONS AND SUGGESTIONS FOR FUTURE WORK 54

6.1 Overall conclusions 54

6.2 Suggestions for future work 58

LIST OF REFERENCES 59

APPENDIX I: UPSEB PLANNING MODEL NETWORK DATA 60

APPENDIX II: IEEE-14 BUS SYSTEM DATA 77

LIST OF FIGURES

Fig.No.	Caption	Page
1.1	Single line diagram of UPSEB planning model network	7
2.1	Thermal turbine and speed governor model	12
2.2	Analog diagram of speed governor and thermal turbine	13
2.3	Hydro turbine and speed governor	16
2.4	Analog diagram of hydro turbine and speed governor	17
3.1	Frequency for equivalent thermal model	26
3.2	Frequency for equivalent hydro model	27
3.3	Frequency for both thermal and hydro representation & frequency for UPSEB system	28
4.1	Equivalent circuit of generator & phasor diagrams for steady state conditions diagra	32
4.2	Vector diagram of synchronous generator in the transient state	33
4.3	Analog diagram of IEEE-1 rotating exciter & IEEE Type-1 rotating excitation system model	36
5.1	Relationships of subroutines for initial conditions & relationships between subroutines during step by step simulation	51
5.2	Single line diagram of IEEE-14 bus system	52
5.3	Frequency for the IEEE-14 bus system	53
6.1	A rotor frequency by transient stability study of the UPSEB system, frequency for both thermal and hydro representation & frequency for UPSEB system	57

LIST OF TABLES

Table No.	Title	Page
2.1	Thermal turbine and speed governor data	18a
2.2	Hydro turbine and speed governor data	18b
5.1	Simulation results for loss of generation on IEEE-14 bus system	50

NOMENCLATURE

E_F	Term representing the field voltage
$\dot{E}_F$	Time derivative of E_F
E_I	Voltage proportional to field current
E_q	Voltage behind quadrature axis synchronous reactance
E'_q	Voltage proportional to field flux linkages due to field and armature currents
$\dot{E}'_q$	Time derivative of E'_q
f	Frequency in Hz
f_o	Nominal operating frequency in Hz
F_{HP}	High pressure turbine power constant
F_{IP}	Intermediate pressure turbine power constant.
F_{LP}	Low pressure turbine power constant
g	Power at gate or valve out-let
g_{min}	Minimum power limit at valve out-let
g_{max}	Maximum power limit at valve out-let
$\dot{g}_{min}$	Lower limit on rate of change of power imposed by gate travel
$\dot{g}_{max}$	Upper limit on rate of chang of power imposed by gate travel
I_T	Terminal current
I_d	Component of I_T referred to machine direct axis
I_q	Component of I_T referred to machine quadrature axis
K_A	Regulator gain

K_E	Exciter constant related to self-excited field
K_F	Regulator stabilizing circuit gain
M_j	Moment of inertia of jth machine
M_T	Total moment of inertia
P_{base}	Base capacity of power of turbine
P_m	Mechanical power output
P_{mj}	Mechanical power output of jth machine
P_{mT}	Total mechanical power
$P_{mT(H)}$	Total mechanical power due to hydel power
$P_{mT(Th)}$	Total mechanical power due to thermal power
$\dot{P}_{mT}$	Time derivative of P_{mT}
P_{es}	Slack machine power
P_{slack}	Slack bus power (real)
P_{ej}	Real power output of jth machine
P_{eT}	Total electrical power output
$P_{eT(H)}$	Total electrical power output of hydro generators
$P_{eT(Th)}$	Total electrical power output of turbo-generators.
r_a	Armature resistance
R	Governor speed regulation constant
S_E	Saturation constant
S_{base}	System base MVA chosen
T_{HP}	Time constant of turbine high pressure section
T_{IP}	Time constant of turbine intermediate pressure section
T_{LP}	Time constant of turbine low pressure section.
T_R	Dash Pot time constant

T_S	Speed governor time constant
T_{DR}	Dash Pot time constant
T_W	Water starting time
T_A	Regulator amplifier time constant
T_E	Exciter time constant
T_F	Regulator stabilizing circuit time constant
T'_{do}	Direct axis transient open circuit time constant
V_T	Terminal voltage of generator
V_{Ref}	Reference voltage setting of exciter regulator control
V_R	Regulator output voltage
V_{Rmin}	Minimum value of V_R
V_{Rmax}	Maximum value of V_R
ω	Angular velocity in Rad/sec.
ω_o	Angular velocity of system centre of inertia Rad/sec.
ω_s	Normal operating speed of the system in Rad/sec.
$\dot{\omega}_o$	Time derivative of ω_o
X_d	Direct axis synchronous reactance
X'_d	Transient reactance
S_q	Quadrature axis synchronous reactance
θ_j	Rotor angle of jth machine with respect to synchronous reference frame
θ_o	System centre angle with respect to synchronous reference frame
$\dot{\theta}_o$	Time derivative of θ_o

$\ddot{\theta}_o$	Derivative of $\dot{\theta}_o = \dot{\omega}_o$
ϕ_j	Angle measured with respect to system centre of inertia
σ	Permanent speed droop constant
δ	Transient speed droop constant.

ABSTRACT

A severe mismatch between generation and demand caused by a sudden change of generation or load can cause the power system frequency to deviate appreciably from its normal value. The system frequency, could fall or increase, dependent upon whether the generation or the load is lost. Of course, the most critical case is the loss of one of the larger generating units of the system. This will lead to under frequency conditions which cannot be tolerated for a long time even if the drop is about 3% from the normal value. If the spinning reserve is also available, the frequency may recover within an acceptable time, otherwise load shedding may have to be done. Obviously, in order to evolve a proper operating strategy, we need to obtain the power-frequency transient upon loss of generation. A common method is by extended transient stability studies. However, such simulation can be computationally very expensive because of small time step involved. In 1971, Stanton proposed 'dynamic energy balance concept' for simulation of power-frequency transients. In this method by avoiding synchronizing oscillations and other small time constants involved with subtransient phenomenon, he claimed a ten to one speed advantage over the conventional transient stability method.

The aim of this thesis is to review the Stanton's scheme in the context of a practical problem faced by a typical electricity board of our country and to develop a model of our own. The test problem chosen is taken from U.P.State Electricity Board planning model network of year 1984-85.

CHAPTER 1

INTRODUCTION

1.1 General Discussion

In power system analysis, the study of 'Power-frequency transients' has gained importance in order to analyse behaviour of various power system components and also the system's behaviour on the whole under abnormal conditions of frequency excursions in the system. It is a well known fact that the frequency of the system is very much dependent on the power balance between generation and demand. Loss of a large block of generation or load will cause a severe mismatch between generation and demand leading to dangerously low or high frequency conditions in the system in few seconds after the occurrence of the disturbance. Under these abnormal frequency conditions, some of the electrical components like synchronous generators, large capacity synchronous motors etc. which are sensitive to frequency changes may loose synchronism causing disastrous conditions in the system. Mechanical vibrations of considerable amplitudes will be induced in the turbine shafts and blades due to the coincidence of their natural frequency modes with the system low frequencies following a loss of large block of generation causing permanent mechanical deformations in the shafts and blades. The modern

turbines must be run at speeds which are very close to synchronous to avoid permanent damage. For example, specifications of 220 MW machines which are being installed in our country now state that the turbines may be damaged permanently even if the speed corresponds to 48 Hz for few minutes.

Following a loss of large block of generation, the redistribution of powers in the network may overload some of the lines already operating at their normal capacity causing line trip out conditions posing a threat to the stability of the system. To avoid such unpleasant situations, the system frequency should be brought back to its normal operating value in minimum amount of time. Large frequency dips can be minimized by fast acting speed-governor mechanisms, by providing spinning reserve in the system and by shedding off the loads using fast acting frequency sensitive relays. The most common practice of restoring system's frequency under these transient conditions is by load shedding. Knowledge about capability of spinning reserve, behaviour of loads at abnormal frequency and voltage conditions will help in developing the most effective load shedding strategies.

Since the disturbance location is most random in nature, exhaustive off-line power-frequency transient studies need to be carried out to develop efficient and

effective load shedding strategies so that minimum number of power consumers are affected. This can involve large amounts of computation effort resulting in excessive costs. So it is highly desirable to have methods which simulate power-frequency transients in an economical way.

1.2 Previous Work

The power-frequency transients resulting from severe mismatches between generation and demand can be simulated by extended transient stability methods. The inclusion of generator subtransient phenomenon, damper bar windings, small excitation time constants set a very low upper limit on time step of integration. However, this can be increased by appropriate choice of dynamic models. Hence the ultimate limit on step size in transient stability studies is the 'frequency of synchronizing oscillations'. However, the ~~duration~~ PERIOD of these oscillations is also very small, a very low step size for integration cannot be avoided. Obviously this results in excessive computation costs for studying power-frequency transients. Even though extended transient stability studies do simulate power-frequency transients, it is primarily meant for simulation of power angle transients which is not our aim.

Recently a new technique of simulation of power-frequency transients has been developed by Stanton [1] using 'Dynamic Energy Balance' concepts. The development of dynamic

energy balance studies is motivated by the need for more economical dynamic simulation of power-frequency transients. The key steps involved in simulation procedure are elimination of synchronizing oscillations, small time constants used in representation of subsystems like excitation, speed governor, turbine and generator models.

During transient conditions, the entire system is assumed to have an equivalent speed 'ω_o' which will be equal to the inertia weighted average of individual generator rotor speeds. This equivalent speed of the system is defined as the velocity of 'system centre of inertia'. The centre of inertia is the rotational analog of centre of mass and is referred as centre of angle 'θ_o'. The centre of angle θ_o is defined as

$$\theta_o = \frac{1}{M_T} \sum_{j=1}^{n} M_j \theta_j \qquad (1.1)$$

where M_j = moment of inertia of jth machine,

θ_j = angle of the jth rotor measured with respect to a synchronously rotating frame of reference

and $M_T = \sum_{j=1}^{n} M_j$ is the total moment of inertia of the system.

n = number of machines present in the system.

The dynamic equations of motion of system centre of inertia are described by the following equations.

$$\frac{d^2\theta_o}{dt^2} = \frac{d\,\omega_o}{dt} = \frac{1}{M_T}(P_{mT} - P_{eT}) \qquad (1.2)$$

and

$$\frac{d\,\theta_o}{dt} = (\omega_o - \omega_s) \qquad (1.3)$$

where P_{mT} = Total mechanical power input to the system,

P_{eT} = Total electrical power output of the system

and ω_s = Synchronous speed of the system.

The frequency 'f' obtained by the solution of equation (1.2) will be the inertia weighted average of frequencies of individual rotors present in the system. The above equations form the basis of simulation of power-frequency transients by dynamic energy balance concepts.

The synchronizing oscillations are eliminated from the simulation method by assuming that the oscillatory power transfers from one rotor to another during these oscillations are zero. These oscillatory power transfers do not significantly effect the total electrical power output P_{eT} of the system. However, they may increase losses slightly. Assumption of P_{eT} constant during these oscillations gives a scope for elimination of synchronizing oscillations from the model. Elimination of these oscillations allows us to choose large time steps for integration and this facilitates to study the slower dynamics of the power system. It has been claimed by Stanton that the simulation of

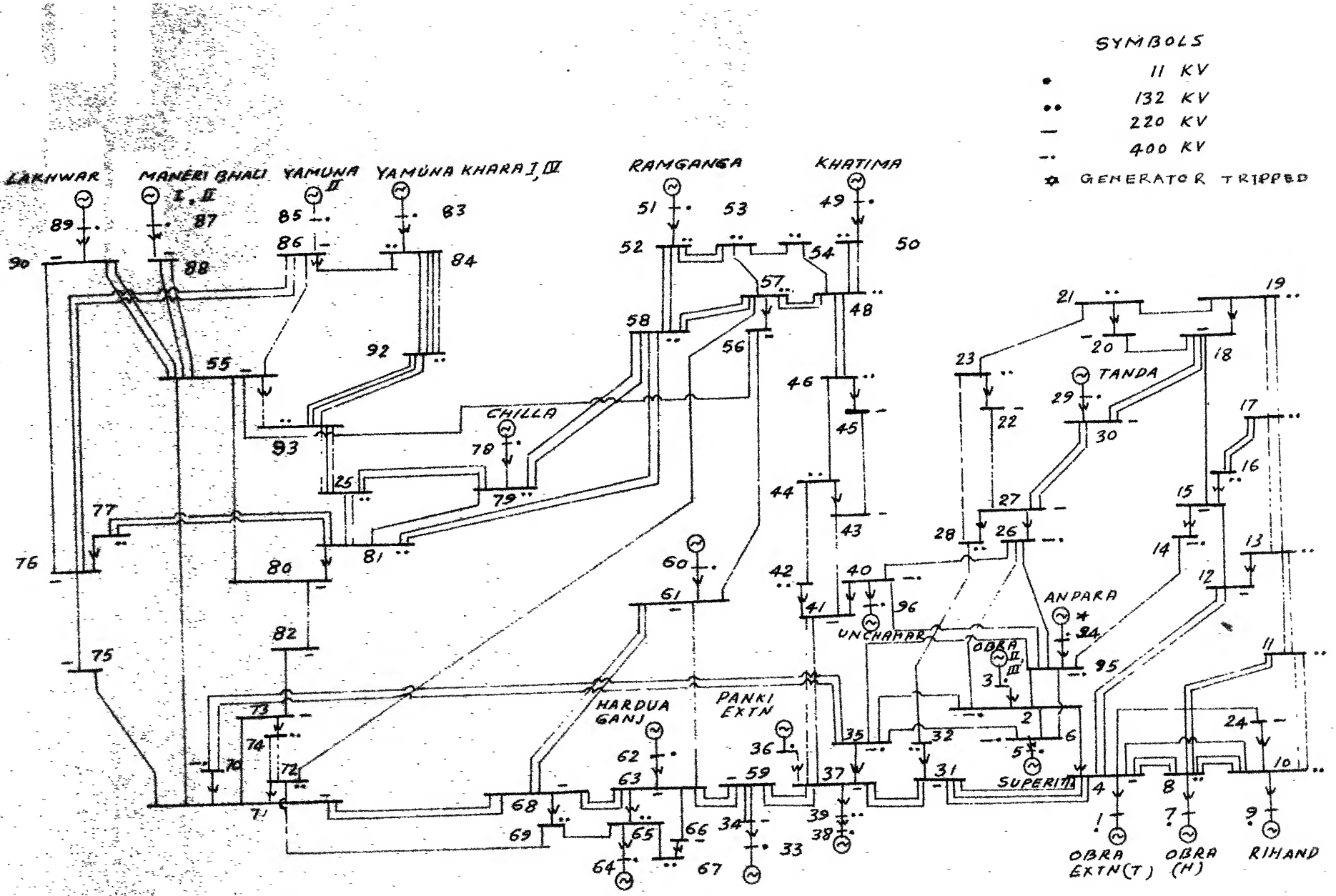

FIG.1-1 SINGLE LINE DIAGRAM OF UPSEB PLANNING MODEL NETWORK

power-frequency transients by this method requires one tenth the computational effort of a transient stability study yet giving similar results within the practical limits.

1.3 Details of Problem under Consideration

It appears from the literature that only Stanton has made a serious effort to develop a method for the study of power-frequency transients. The aim of this thesis is to review this method in the context of a practical problem faced by a typical electricity board of our country and develop a suitable model of our own.

The problem chosen is taken from U.P.State Electricity Board planning model network for the year 1984-85. A single line diagram of the planned network is given in Fig. 1.1.* It consists of 20 generators, 96 buses and 136 lines. The number of buses is not too large as only high voltage network is considered. Out of these 20 generating stations, there are 11 thermal and 9 hydro stations. The total MVA capacity of the system is 7576 out of which 1790 MVA is hydro and the rest, i.e. 5786 MVA is thermal. The objective is to study the power-frequency transient if 528 MVA thermal generator at Anpara is tripped. This particular generator, prior to the trip out is assumed to be delivering 400 MW power. The total spinning reserve available at the time of the trip out is assumed to be 560 MVA.

*The bus data prior to disturbance, line, transformer, shunt load and voltage controlled bus data is given in Appendix I.

The chapterwise description of the thesis is given below.

The second chapter deals with the speed governor and turbine models.

The third chapter covers the simulation of power-frequency transients treating electrical loading as constant.

The fourth chapter deals with the generator and excitation models.

The fifth chapter deals with the simulation of power-frequency transients considering the electrical loading.

Overall conclusions and suggestions for future work are projected in the last chapter.

CHAPTER 2

TURBINE AND SPEED GOVERNOR MODELS

2.1 General Discussion

Before we can study the power-frequency transient problem of the system described in Sec. 1.3, we need to get acquainted with the models for hydro and steam turbines and speed governing mechanisms. Therefore, they are discussed first as given below from Ref. [2].

2.2 Speed Governor and Thermal Turbine Model

The block diagram model representation of speed governor and thermal turbine are given in Fig.2.1. In the speed governor block, the meaning of various quantities is as follows:

ω_{ref} = Reference speed, rad/sec.

ω = Actual speed, rad/sec.

R = Speed regulation constant of speed governor

f_o = Normal operating frequency, Hertz

T_s = Speed governor time constant, seconds

$\dot{g}_{min}$ = Lower limit on rate of change of power imposed by control valve rate limits

$\dot{g}_{max}$ = Upper limit on rate of change of power imposed by control valve rate limits

g_{min} = Lower limit imposed by valve travel

g_{max} = Upper limit imposed by valve travel

g = Valve position, p.u.

Similarly the meaning of various symbols used for the turbine block are

T_{HP}, T_{IP}, T_{LP} = Time constants of high pressure, intermediate pressure, low pressure stages respectively in seconds

F_{HP}, F_{IP}, F_{LP} = Fractional power coefficients of high pressure, intermediate pressure and low pressure stages respectively

$F_{HP}+F_{IP}+F_{LP}$ = 1

P_{base} = Turbine MVA rating

S_{base} = System base MVA

P_m = Mechanical power, p.u.

The analog diagram representation of Fig.2.1 is shown in Fig.2.2. The analog representation helps in writing the appropriate dynamic equations for digital computer solution as given below. For calculation of initial conditions, the following equations are used.

$$g = (P_m . S_{base})/P_{base}(F_{HP}+F_{IP}+F_{LP}) \qquad (2.1)$$

$$\omega_{ref} = \omega_o + (g.R.2\pi f_o) \qquad (2.2)$$

$$X_4 = g \qquad (2.3)$$

$$X_5 = g \qquad (2.4)$$

$$X_6 = g \qquad (2.5)$$

$$X_7 = g \qquad (2.6)$$

During step by step integration procedure, the following equations are used

$$g = X_4 \quad , \quad g_{min} \leq X_4 \leq g_{max} \tag{2.7}$$

$$X_1 = (\omega_{ref} - \omega)/(R.2\pi f_o) \tag{2.8}$$

$$X_2 = (X_1 - g)/T_s \tag{2.9}$$

$$X_3 = X_2 \quad , \quad \dot{g}_{min} \leq X_2 \leq \dot{g}_{max} \tag{2.10}$$

$$\dot{X}_4 = X_3 \tag{2.11}$$

Equations (2.7) to (2.11) discribe the performance of the speed governor.

The solution of differential equation (2.11) gives the position of the effective controlled governor valve symbolised as g. This becomes the input to the turbine.

The turbine equations are

$$\dot{X}_5 = (g - X_5)/T_{HP} \tag{2.12}$$

$$\dot{X}_6 = (X_5 - X_6)/T_{IP} \tag{2.13}$$

$$\dot{X}_7 = (X_6 - X_7)/T_{LP} \tag{2.14}$$

and $$P_m = (F_{HP}.X_5 + F_{IP}.X_6 + F_{LP}.X_7) \frac{P_{base}}{S_{base}} \tag{2.15}$$

In the above equations, the differential equations are represented as $\dot{X} = dX/dt$. The differential equations (2.11) to (2.14) are solved at each integration time step by making use of equations (2.7) to (2.10) to get the mechanical power output of the turbine P_m.

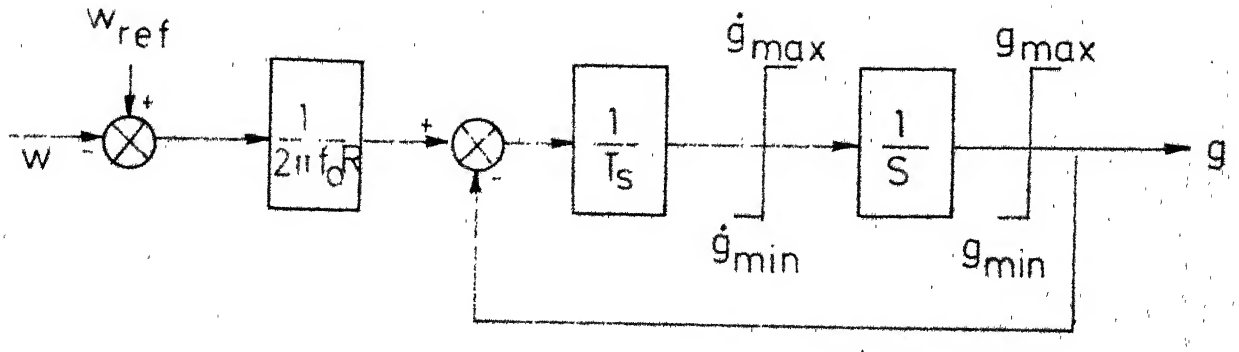

SPEED GOVERNOR

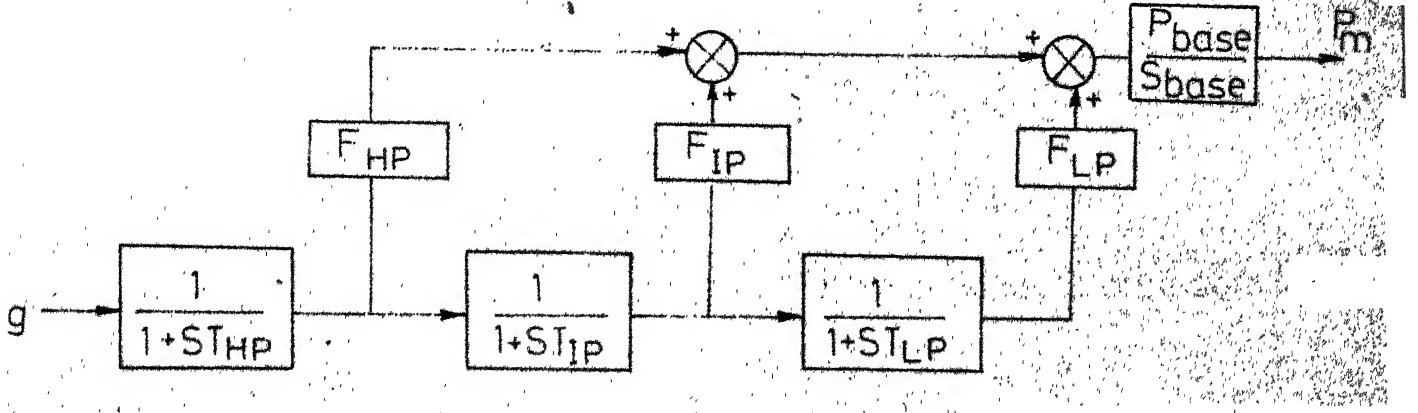

TURBINE

FIG 21 THERMAL TURBINE AND SPEED GOVERNOL MODEL

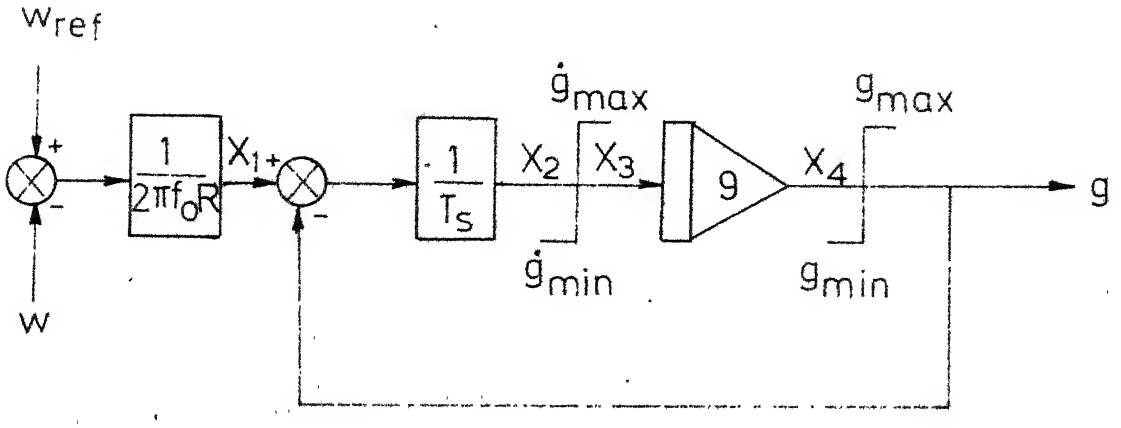

SPEED GOVERNOR

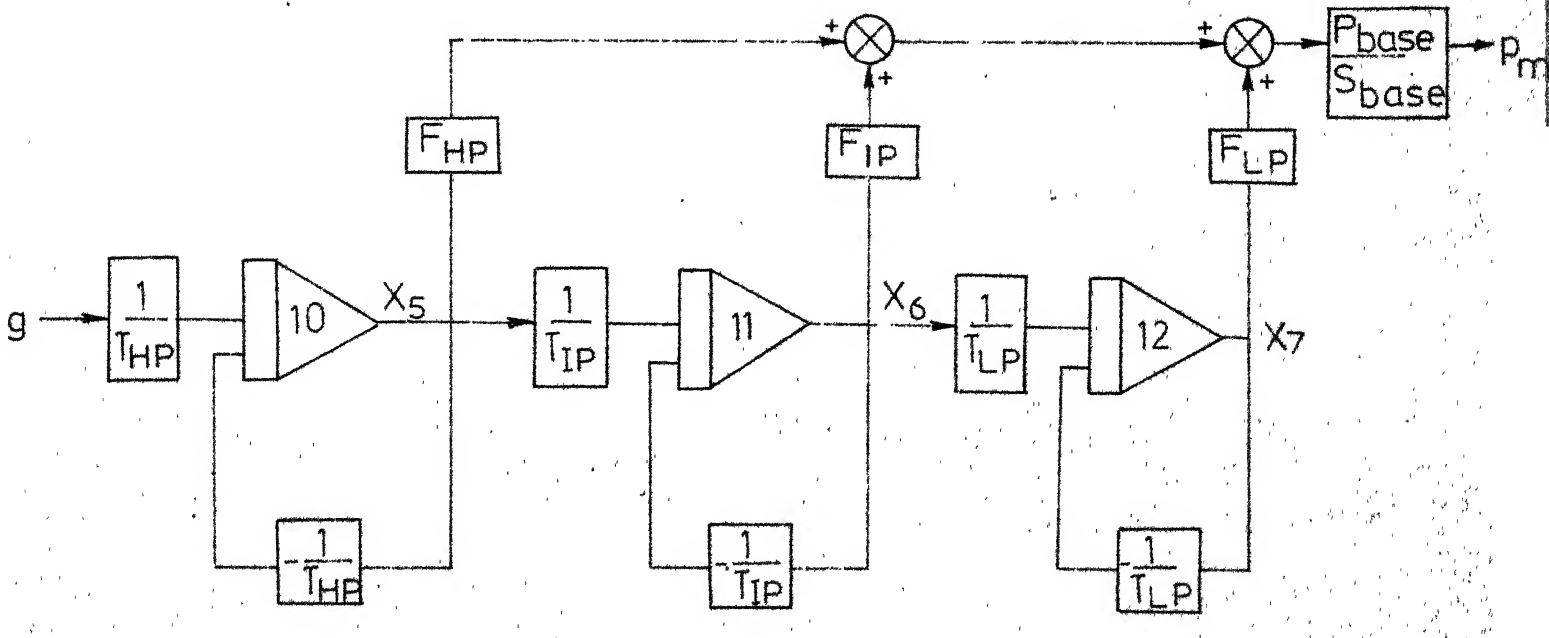

TURBINE

FIG. 2.2 ANALOG DIAGRAM OF SPEED GOVERNOR AND THERMAL TURBINE

2.3 Speed Governor and Hydro Turbine Model

The block diagram representation of the hydro speed governor and turbine are given in Fig.2.3. In the speed governor block, the various symbols have the following meaning.

ω_{ref}, ω, T_s, $\dot{g}_{min}$, $\dot{g}_{max}$, g_{min}, g_{max}, g

have similar meaning as given in Sec. 2.2.

T_R = Dash pot time constant, seconds

σ = Permanent speed droop coefficient

δ = Transient speed droop coefficient

Similarly the meaning of various symbols used in the turbine block are

T_W = Water starting time, seconds

P_{base} = Turbine MVA rating

S_{base} = System base MVA chosen.

The analog diagram representation of Fig.2.3 is shown in Fig. 2.4 from which the following equations are written. The initial conditions are calculated by the following equations.

$$X_4 = P_m \frac{S_{base}}{P_{base}} \tag{2.16}$$

$$X_5 = X_4 . \delta \tag{2.17}$$

$$X_7 = 1.5\, X_4 \tag{2.18}$$

$$\omega_{ref} = \omega_o + (X_4 . \sigma . 2\pi f_o) \tag{2.19}$$

During step by step integration, the following equations are used

$$g = X_4 \quad , \quad g_{min} \leq X_4 \leq g_{max} \tag{2.20}$$

$$X_1 = (\omega_{ref} - \omega)/2\pi f_o \tag{2.21}$$

$$X_6 = g.\delta - X_5 \tag{2.22}$$

$$X_2 = (X_1 - X_6 - g\,.\sigma\,)/T_s \tag{2.23}$$

$$X_3 = X_2 \quad , \quad \dot{g}_{min} \leq X_2 \leq \dot{g}_{max} \tag{2.24}$$

$$X_8 = 2.0(X_7 - g) \tag{2.25}$$

$$\dot{X}_4 = X_3 \tag{2.26}$$

$$\dot{X}_5 = X_6/T_R \tag{2.27}$$

$$\dot{X}_7 = (g - X_8)/T_W \tag{2.28}$$

$$\text{and } P_m = X_8 \frac{P_{base}}{S_{base}} \tag{2.29}$$

In the above equations the differential equations (2.26) to (2.28) are solved at each integration time step by making use of equations (2.20) to (2.25) to get the mechanical power output of the turbine, P_m.

2.4 Turbine and Speed Governor Data for the UPSEB System

The system has 20 machines out of which the turbine data is available for only 16 machines. The remaining 4 are treated as constant mechanical power output turbines throughout the simulation period.

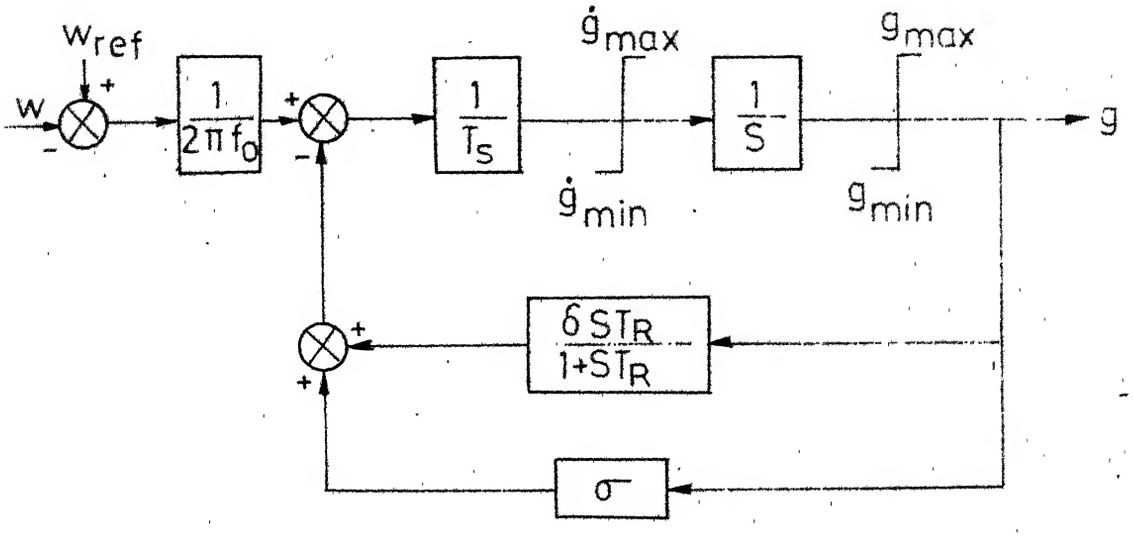

SPEED GOVERNOR

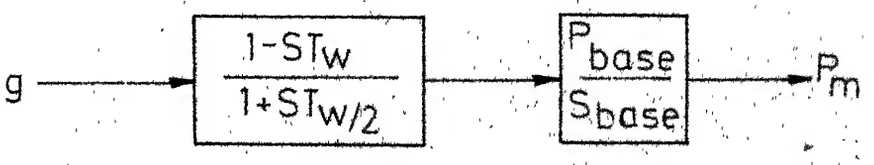

HYDRAULIC TURBINE

FIG. 23 HYDRO TURBINE AND SPEED GOVERNOR

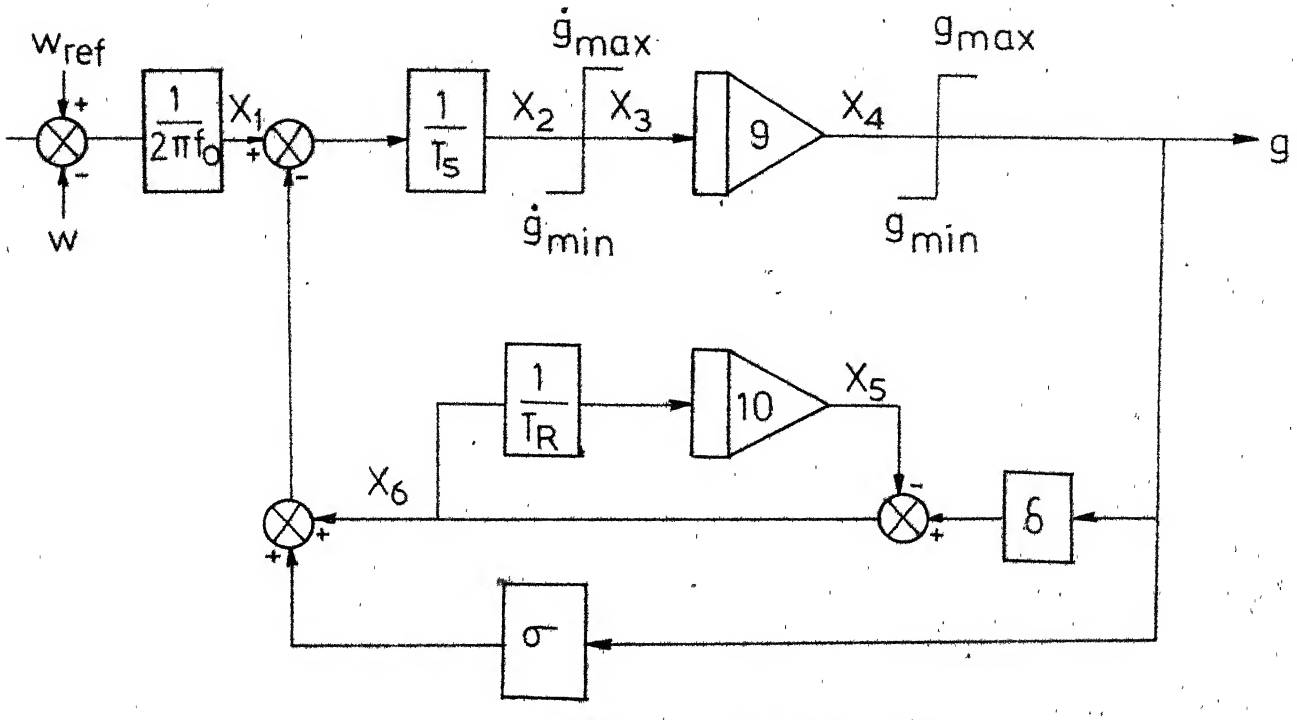

SPEED GOVERNOR

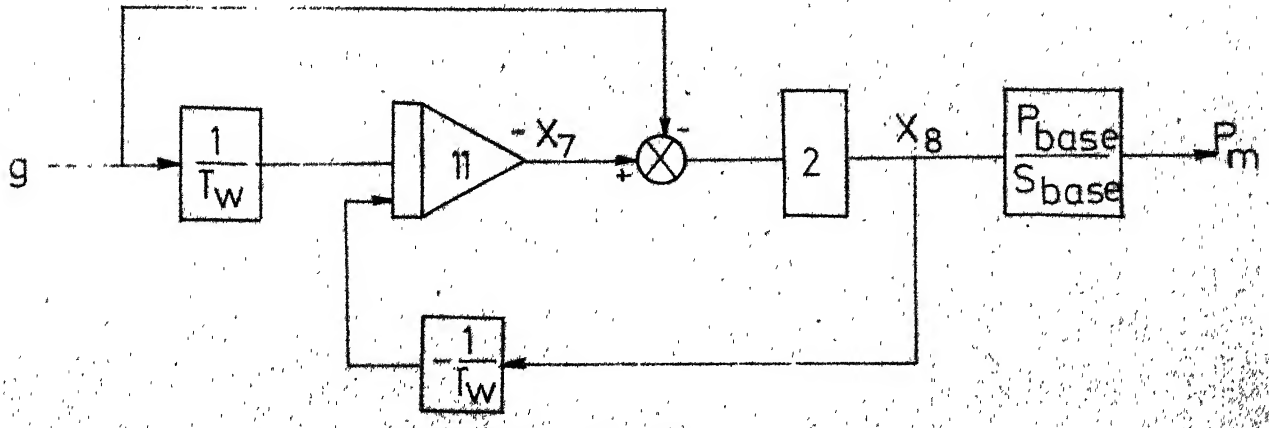

TURBINE

FIG. 2-4 ANALOG DIAGRAM OF HYDRO TURBINE AND SPEED GOVERNOR

The data for thermal turbines and speed governors is given in Table 2.1 and the data for hydro turbines and speed governors is given in Table 2.2.

Table 2.1: Thermal Turbine and Speed Governor Data.

No.	P_{base}	T_{HP}	T_{IP}	T_{LP}	F_{HP}	F_{IP}	F_{LP}	R	T_S	$\dot{g}_{min}$	$\dot{g}_{max}$	g_{min}	g_{max}
1	940	0.2	4.0	1000.0	0.62	0.38	0.0	0.04	0.425	-1.18	0.59	0.0	0.80
2	422	0.2	4.0	1000.0	0.61	0.39	0.0	0.04	0.425	-1.18	0.59	0.0	0.77
‡3	940												
4	275	0.2	10.0	1000.0	0.26	0.74	0.0	0.04	0.425	-1.18	0.59	0.0	0.74
5	139	0.2	10.0	1000.0	0.26	0.74	0.0	0.04	0.425	-1.18	0.59	0.0	0.78
6	217	0.2	10.0	1000.0	0.26	0.74	0.0	0.04	0.425	-1.18	0.59	0.0	0.74
*7	528												
8	340	0.2	4.0	1000.0	0.62	0.38	0.0	0.04	0.425	-1.18	0.59	0.0	0.84
9	75	0.2	4.0	1000.0	0.62	0.38	0.0	0.04	0.425	-1.18	0.59	0.0	0.74
10	1420	0.15	0.74	9.0	0.24	0.0	0.76	0.05	0.03	-100.0	100.0	0.0	0.83
11	490	0.2	4.0	1000.0	0.62	0.38	0.0	0.04	0.425	-1.18	0.59	0.0	0.78

* This machine is tripped out.

‡ Constant power output turbine.

Table 2.2: Hydro Turbine and Speed Governor Data.

No.	P_{base}	T_W	T_S	T_R			$\dot{g}_{min}$	$\dot{g}_{max}$	g_{min}	g_{max}
1	110	1.63	0.015	12.0	0.04	0.36	-0.2	0.1	0.0	0.90
2	335	1.0	0.015	5.0	0.04	0.30	-0.2	0.1	0.0	0.90
3	51	1.0	0.015	5.0	0.04	0.30	-0.2	0.1	0.0	0.80
4	220	1.0	0.015	5.0	0.04	0.30	-0.2	0.1	0.0	0.91
5	211	1.0	0.015	5.0	0.04	0.30	-0.2	0.1	0.0	0.91
6	376	1.11	0.02	12.0	0.04	0.36	-0.1	0.05	0.0	0.945
*7	103									
*8	160									
9	223	1.1	0.02	10.0	0.04	0.3	-0.2	0.1	0.0	0.92

* Constant power output turbine.

CHAPTER 3

IMPLEMENTATION TREATING ELECTRICAL LOADING AS CONSTANT

3.1 General Discussion

To get a 'feel' of the problem posed in Sec. 1.3, it was decided that at first we would not get involved with the electrical network and generator characteristics. Thus for the time being we shall assume that after the disturbance, the electrical loading is not changed and therefore the total load requirement plus the network losses stay constant. The moment the disturbance occurs, obviously the total output of the generation is less than the load requirement. This will result in lower speed than the synchronous value. This would inturn activate the speed governor mechanism to increase the mechanical power output of the turbines whenever spinning reserve is available. Since in the problem under consideration, adequate spinning reserve of 560 MVA compared to the generation drop of 400 MW is available, eventually the system generation will match the system load plus the network losses. This problem was analysed in four parts as follows.

Part -(a): It was assumed that the entire generation is thermal and it would be represented by one equivalent thermal turbine.

Part - (b): It was assumed that the entire generation is hydro and it could be represented by one equivalent hydro turbine.

Part-(c): The system is represented by both the equivalent thermal and hydro turbines. All the hydro stations are represented by a single equivalent hydro turbine and all the thermal stations by a single equivalent thermal turbine.

Part - (d): In this part of study, each power station is represented by an equivalent hydro or thermal turbine as the case may be. Identity of all the power stations in the system is retained.

3.2 Implementation

Part - (a):

The MVA rating of the equivalent thermal turbine is assumed to be equal to the sum of MVA ratings of individual power stations and is equal to 7576.25. It was observed from the data given in Table 2.1 that all the speed governers of the machines have similar characteristics, and also for the most of the turbines, the characteristics of high pressure, intermediate pressure and low pressure stages are similar. From these observations, the following data has been chosen for the equivalent thermal turbine.

P_{base} = 7565.25 MVA T_{HP} = 0.2 seconds

T_{IP} = 4.0 seconds T_{LP} = 1000.0 seconds

$F_{HP} = 0.62$ $\quad F_{IP} = 0.38$

$F_{LP} = 0.0$ $\quad R = 0.04$

$T_s = 0.425$ seconds $\quad \dot{g}_{min} = -1.18$

$\dot{g}_{max} = 0.59$ $\quad g_{min} = 0.0$ and $g_{max} = 0.8$.

From the initial load flow conditions prior to the disturbance, the total electrical power output of the system is calculated by

$$P_{eT} = \sum_{j=1}^{n} P_{ej} \tag{3.1}$$

and is equal to 5556.87 MW

P_{ej} = Electrical power output of the jth machine

n = Number of machines = 20

Similarly the total mechanical power input to the system is computed by

$$P_{mT} = \sum_{j=1}^{n} P_{mj} \tag{3.2}$$

where $P_{mj} = P_{ej}$

The system equations of motion are given by

$$\frac{d\,\omega_o}{dt} = \frac{1}{M_T}(P_{mT} - P_{eT}) \tag{3.3}$$

where M_T and ω_o are defined in Sec.1.2 and

$$\dot{P}_{mT} = F(P_{mT}, \omega_o) \tag{3.4}$$

The equivalent thermal turbine dynamical equations described in Sec. 2.2 are written symbolically in the form of equation (3.4). During each time step, the equations (3.3) and (3.4) are solved together by using Runge-Kutta Fourth Order method to obtain the frequency of the system given by the equation

$$f = \omega_o/2\pi \qquad (3.5)$$

The frequency is plotted against time and is shown in Fig.3.1.

Part - (b):

The following test data has been chosen for the equivalent hydro turbine on the basis of the similar observations discussed in part (a).

P_{base}	= 7576.25 MVA	T_W	= 1.63 seconds
T_S	= 0.015 seconds	T_R	= 12.0 seconds
σ	= 0.04	δ	= 0.36
$\dot{g}_{min}$	= -0.2	$\dot{g}_{max}$	= 0.1
g_{min}	= 0.0	g_{max}	= 0.9

The simulation procedure is similar as given in Sec. 3.2, Part (b). The dynamical equations of hydro turbine and speed governor are described in Sec. 2.3.

The frequency versus time graph is shown in Fig.3.2.

Part - (c):

The MVA rating of the equivalent thermal turbine is assumed to be equal to the sum of MVA ratings of the individual thermal power stations and is equal to 5786.0. Similarly the MVA rating of the equivalent hydro turbine is equal to the sum of MVA ratings of the individual hydro power stations.* The total load on the system is 5556.87 MW. The same data given in Part-(a) and Part-(b) is used for the equivalent thermal and hydro turbines respectively. From the initial load flow data prior to the disturbance, total electrical power outputs of thermal and hydrogenerators are computed and are symbolised as $P_{eT(Th)}$ and $P_{eT(H)}$. Now the total electrical power output of the system is

$$P_{eT} = P_{eT(Th)} + P_{eT(H)} \tag{3.6}$$

Similarly the total mechanical power input to the system is given by

$$P_{mT} = P_{mT(Th)} + P_{mT(H)} \tag{3.7}$$

The equations of motion of the system are

$$\frac{d\omega_o}{dt} = \frac{1}{M_T}(P_{mT} - P_{eT}) \tag{3.8}$$

$$\dot{P}_{mT(Th)} = F(P_{mT(Th)}, \omega_o) \tag{3.9}$$

and $$\dot{P}_{mT(H)} = F(P_{mT(H)}, \omega_o) \tag{3.10}$$

where equations (3.9) and (3.10) are symbolic representations of the dynamic equations of thermal and hydro turbines given

* and is equal to 1790 MVA.

in Sec. 2.2 and Sec.2.3 respectively. At each time step of integration , equations (3.8) to (3.10) are solved together using Runge-Kutta Fourth Order integration method. The graph of frequency versus time is shown in Fig.3.3.

Part - (d):

For this case study, the turbine data used is given in Tables 2.1 and 2.2. Since all the turbines are represented by their respective speed governor controls, the dynamic equations of speed governor and turbines are written in the form

$$\dot{P}_{mj} = F(P_{mj}, \omega_o) \quad \text{where } j = 1,2,\ldots,n \qquad (3.11)$$

equations of motion of the system are solved at each time step by using Runge-Kutta Fourth order integration method. The frequency is plotted against time and is also shown in Fig. 3.3.

3.3 Discussion and Conclusions

It should be apparent that the results obtained in Part-(a) and Part-(b) cannot be close to the actual results. Representation of the system by one equivalent thermal or hydro machine was carried out in order to examine the relative performances of a purely thermal and a purely hydro system. It is observed from Figs. 3.1 and 3.2 that a thermal system can pick up the load much faster compared to the hydro system. As seen from Fig.3.1, for a

thermal system, the frequency dropped only by about 0.62 Hz. The minimum frequency condition occurred in less than 4 seconds and reached the steady state value in about 16 seconds. On the other hand, for the hydro system, the frequency had gone down to as low as 47 Hz in less than 4 seconds and the oscillatory conditions continued to prevail as long as the duration of the study which is 40 seconds. This is because of high moment of inertia of the hydro turbines and also large time constants involved in the system dynamics.

If we examine Fig.3.3, it is seen that the behaviour of frequency of the system is in between Figs. 3.1 and 3.2 with no oscillatory behaviour. It was also observed that the representation of the entire system by one equivalent thermal and one equivalent hydro machine gave results very close to the one where the identity of all the power stations were retained (Part - d). This is due to the fact that most of the thermal as well as hydro machines have similar characteristics.

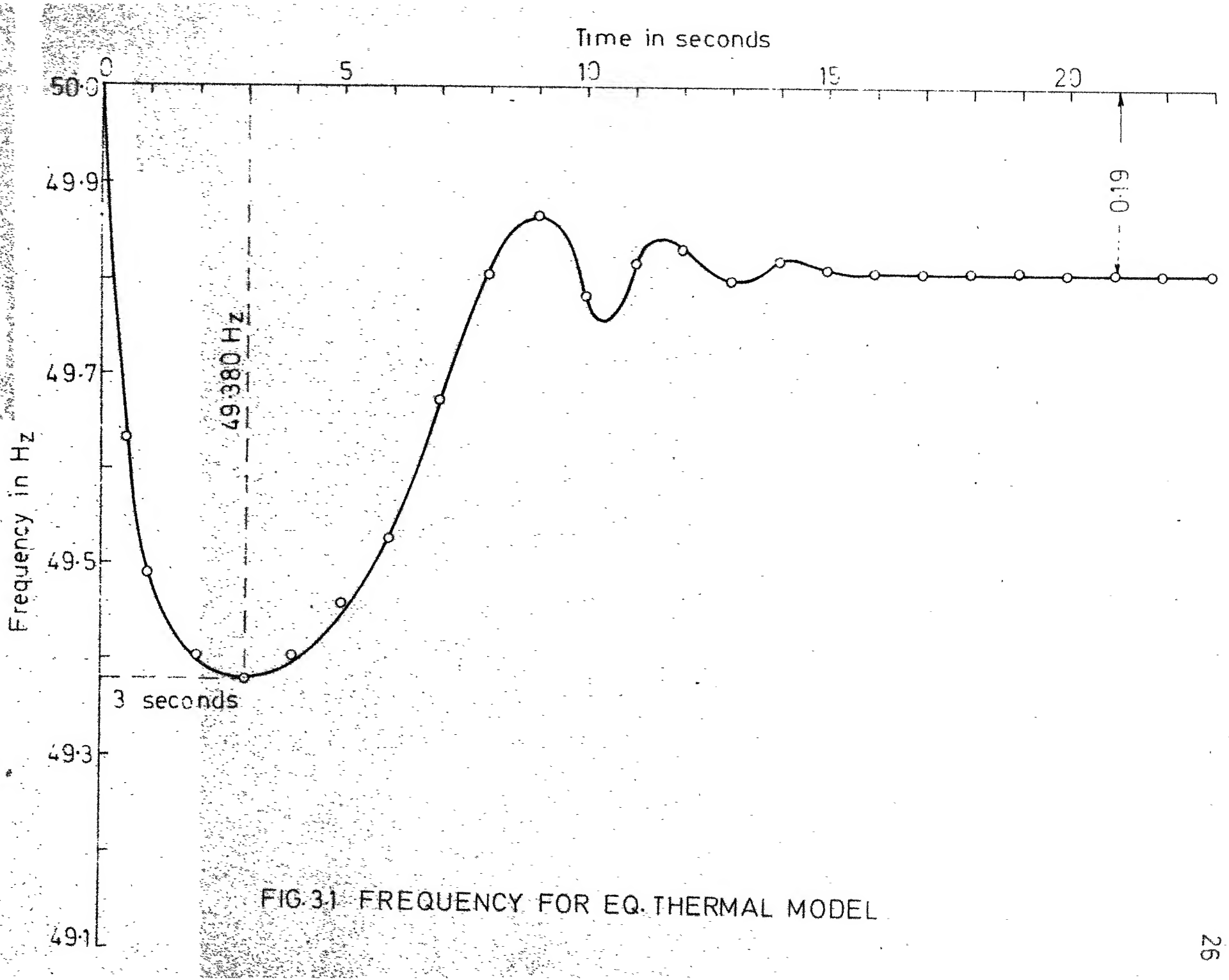

FIG 3.1 FREQUENCY FOR EQ. THERMAL MODEL

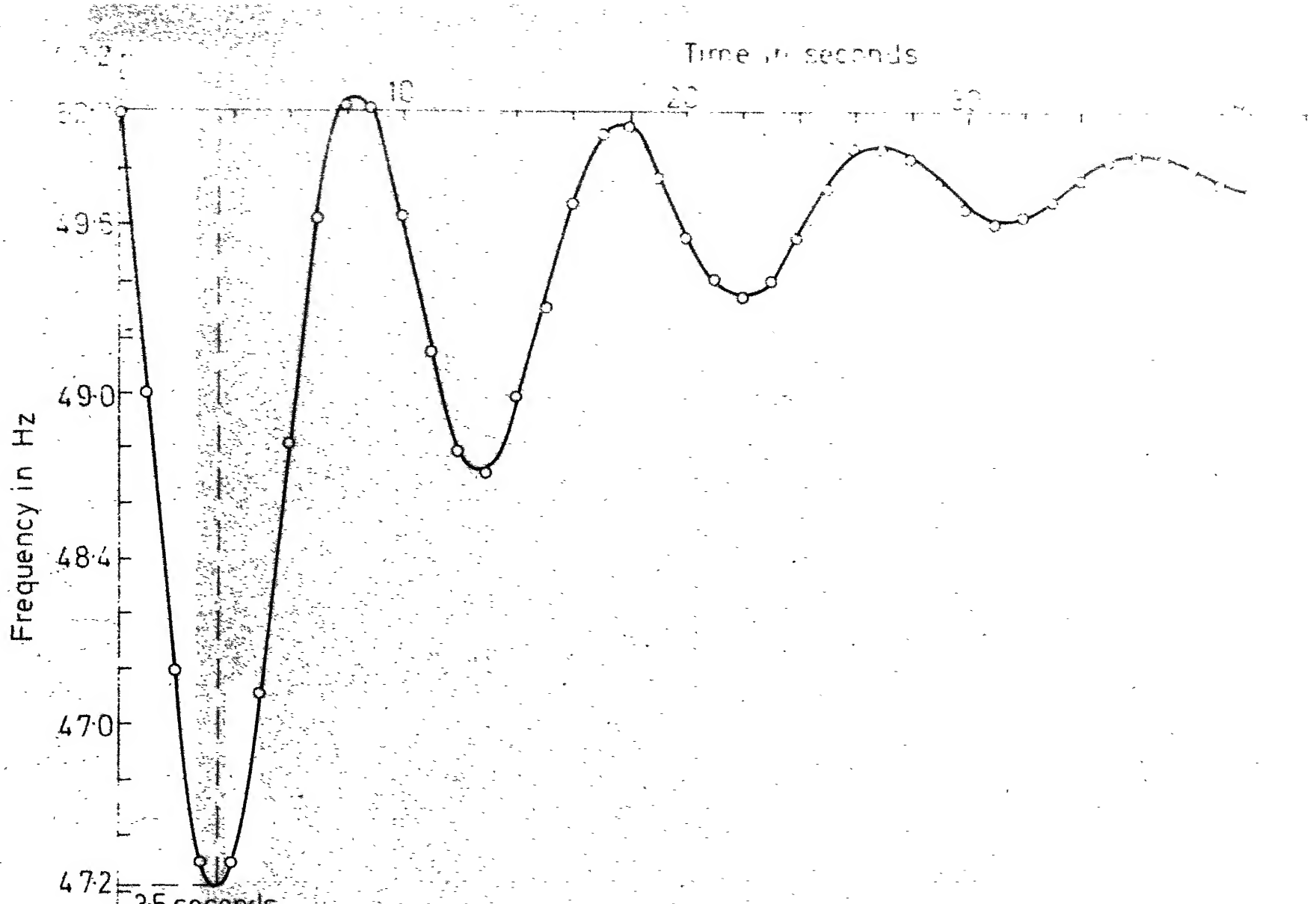

FIG 3.2 FREQUENCY FOR EQ. HYDRO MODEL

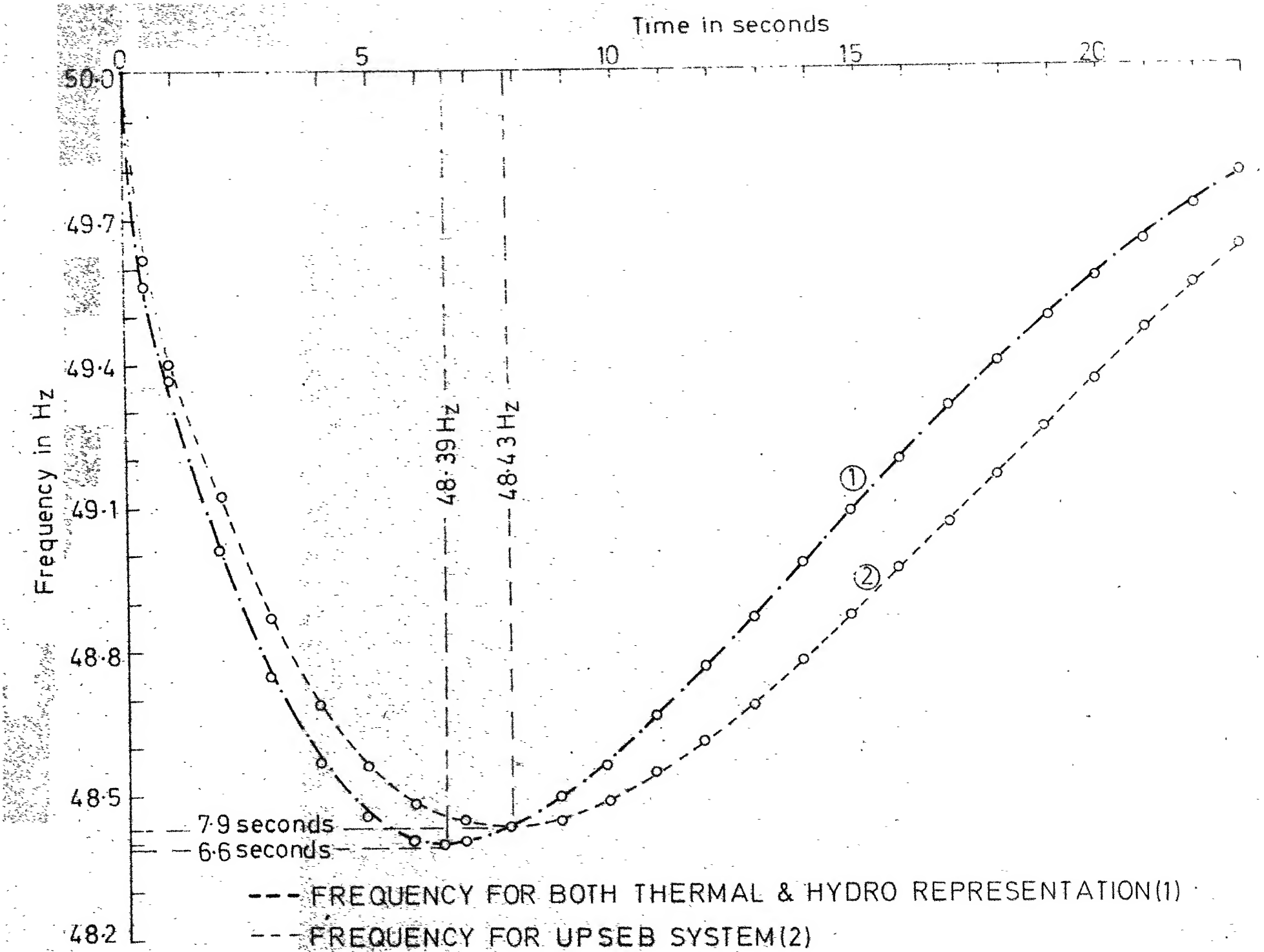
Time in seconds
0
5
10
15
20
50·0
49·7
49·4
49·1
48·8
48·5
48·2
Frequency in Hz
48·39 Hz
48·43 Hz
7·9 seconds
6·6 seconds
①
②
--- FREQUENCY FOR BOTH THERMAL & HYDRO REPRESENTATION(1)
--- FREQUENCY FOR UPSEB SYSTEM(2)

FIG.3.3

CHAPTER 4

GENERATOR AND EXCITATION SYSTEM MODELS

4.1 Generator Representation

A simplified generator representation is used by eliminating damper bar windings and other subtransient effects [3]. Because of elimination of synchronising oscillations, which is discribed in Sec. 1.2, relative movement between the rotor and airgap flux wave is not rapid enough nor of sufficient magnitude to induce currents in the damper bar windings. Hence the damper bar winding is not represented in the model. The changes in field flux linkages are taken into account. With conventional d-q representation of the machine, only field winding is assumed to be on the d-axis. The quadrature axis is chosen to lead the direct axis by 90 electrical degrees. The position of the quadrature axis is determined by calculating a fictitious voltage located on this axis. This is a voltage back of quadrature axis synchronous reactance X_q and is determined by the equation (4.1)

$$E_q = V_T + (r_a + jX_q)I_T \qquad (4.1)$$

where E_q = Voltage behind quadrature axis synchronous reactance.

V_T = Terminal voltage of the generator.

I_T = Terminal current of the generator.

r_a = Stator resistance

and X_q = Quadrature-axis synchronous reactance.

The equivalent circuit of the generator and the phasor diagrams for steady state conditions are shown in Fig.4.1.

The voltage induced by the field flux will be in phase with the quadrature axis and this voltage can be determined by the equation

$$E_I = V_T + r_a I_T + jX_d I_d + jX_q I_q \qquad (4.2)$$

where I_d and I_q are direct and quadrature axis components of terminal current I_T respectively. The quadrature axis component of voltage back of transient reactance X'_d is given by

$$E'_q = E_q - j(X_q - X'_d)I_d \qquad (4.3)$$

where E'_q = Voltage proportional to field flux linkages resulting from the combined effect of field and armature currents.

X'_d = Direct axis transient reactance and

I_d = Direct axis component of terminal current I_T.

Since field flux linkages do not change instantaneously, E'_q also does not change instantaneously. The rate of change of E'_q along the quadrature axis is dependent on the field voltage controlled by the regulator and exciter, the voltage proportional to field current and direct axis

transient open circuit time constant and is given by the expression

$$\frac{d\,E'_q}{dt} = \frac{1}{T'_{do}}(E_F - E_I) \qquad (4.4)$$

where E_F = Field voltage acting along the quadrature axis

E_I = Voltage proportional to field current and

T'_{do} = Direct-axis transient open circuit time constant, seconds.

The detailed phasor diagram describing E_q, E_I and E'_q is given in Fig. 4.1.

$$E_I = E'_q + (X_d - X'_d)I_d \qquad (4.5)$$

and $$E_q = E'_q + (X_q - X'_d)I_d \qquad (4.6)$$

The above equations (4.4) to (4.6) represent the generator behaviour under transient state. The transient state vector diagram is shown in Fig.4.2.

4.2 Excitation System Model

The excitation system is represented by IEEE type-1 rotating exciter model [4]. The block diagram is shown in Fig. 4.3. Various symbols used in the block diagram carry the following meanings.

V_{Ref} = Regulator reference voltage setting, p.u.

V_T = Generator terminal voltage, p.u.

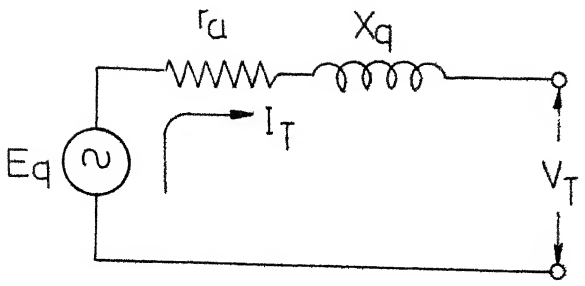

EQ. CIRCUIT OF GENERATOR

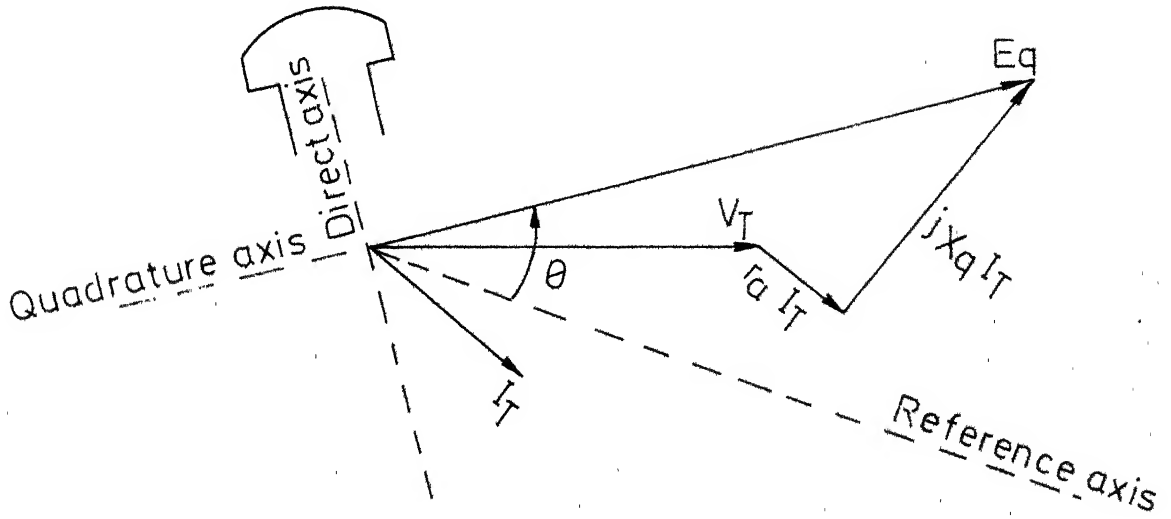

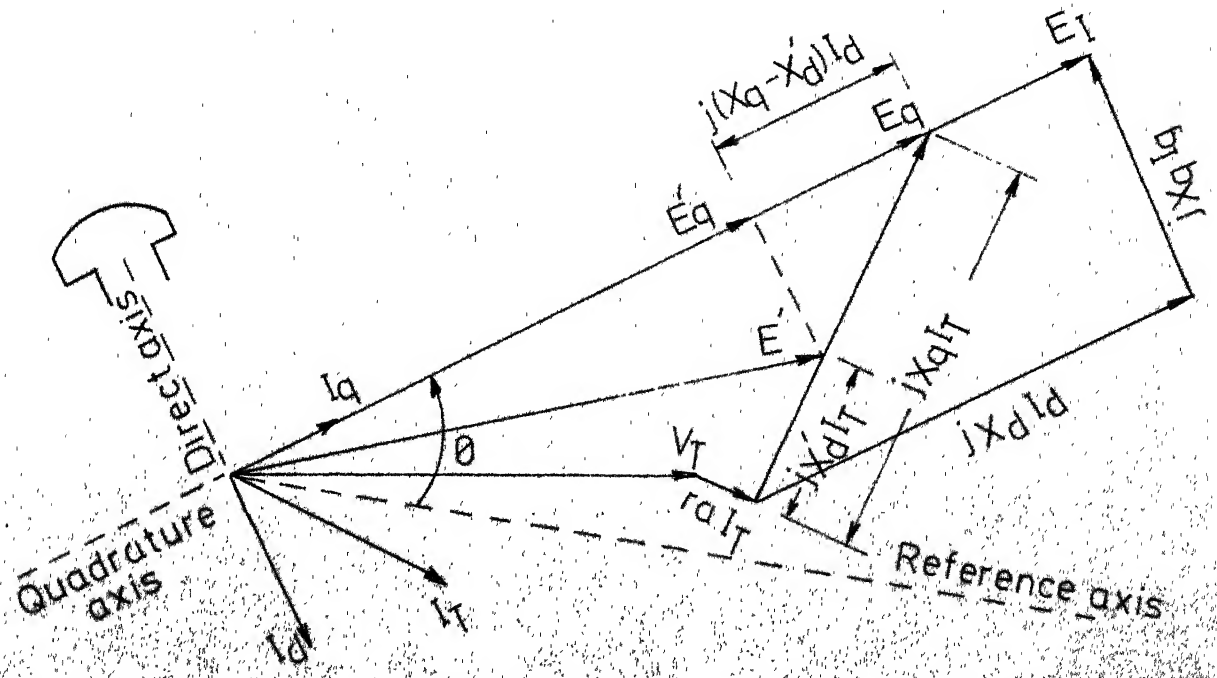

PHASOR DIAGRAMS FOR STEADY STATE CONDITIONS

FIG. 41

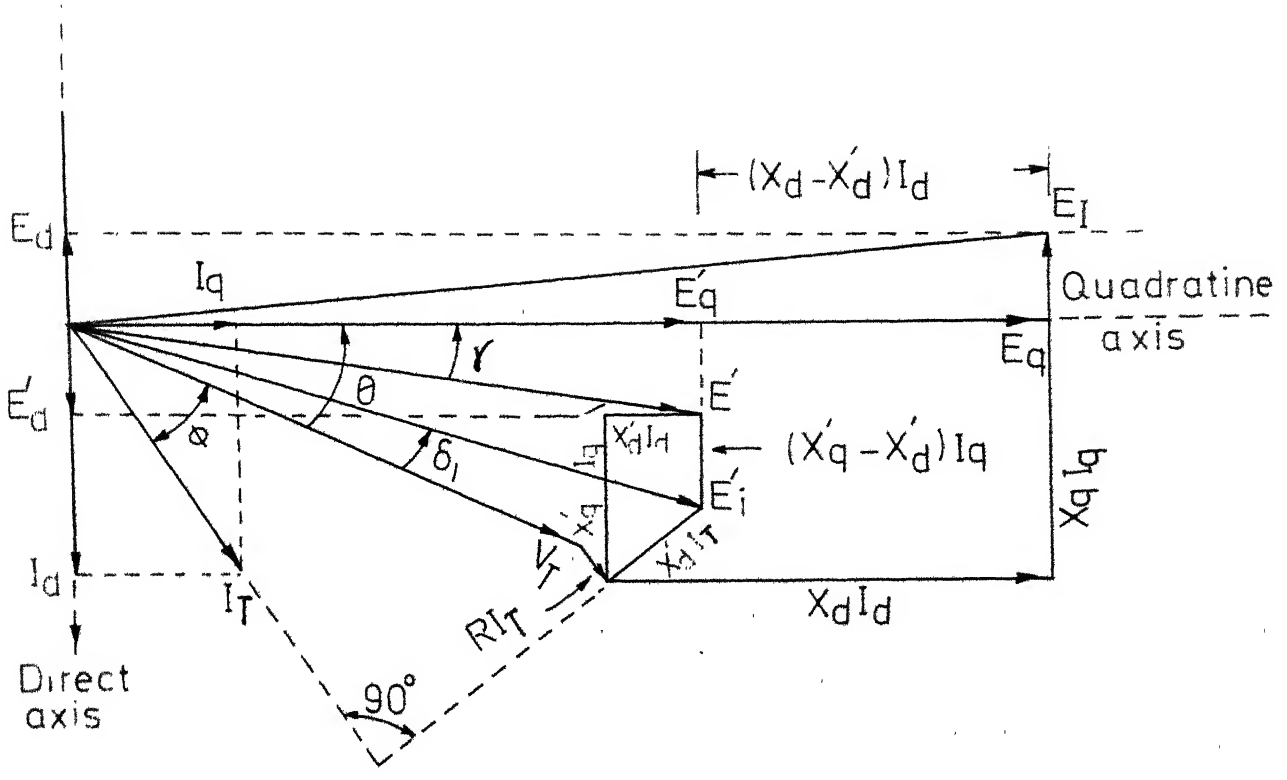

FIG. 4.2 VECTOR DIAGRAM OF SYNCHRONOUS GENERATOR IN THE TRANSIENT STATE

K_A = Regulator gain

T_A = Regulator amplifier time constant, seconds

$V_{R\ max}$ = Maximum value of regulator output voltage

$V_{R\ min}$ = Minimum value of regulator output voltage

K_E = Exciter constant related to self excited field

T_E = Exciter time constant, seconds

K_F = Regulator stabilizing circuit gain

T_F = Regulator stabilizing circuit time constant, seconds

S_E = Exciter saturation function

A,B = Exciter saturation constants.

The analog representation of excitation system is also shown in Fig.4.3, from which the dynamic equations for digital computer solution are written. For calculating initial conditions, the following equations are used.

$$X_5 = E_F(K_E + S_E) \tag{4.7}$$

$$X_3 = E_F \frac{K_F}{T_F} \tag{4.8}$$

$$V_{Ref} = V_T + (K_E + S_E)E_F/K_A \tag{4.9}$$

The initial field voltage, E_F, is set equal to E_I calculated from equation (4.2). During step by step integration the following equations are used,

$$X_1 = V_{Ref} - V_T \tag{4.10}$$

$$X_2 = \frac{K_F}{T_F} E_F - X_3 \tag{4.11}$$

$$X_4 = X_1 - X_2 \tag{4.12}$$

$$X_6 = X_5 \quad , \quad V_{R\,min} \leq X_5 \leq V_{R\,max} \tag{4.13}$$

$$X_7 = E_F\, S_E \tag{4.14}$$

$$X_8 = X_6 - X_7 \tag{4.15}$$

$$\dot{E}_F = \frac{X_8}{T_E} - \frac{K_E}{T_E} E_F \tag{4.16}$$

$$\dot{X}_5 = \frac{K_A}{T_A} X_4 - \frac{X_5}{T_A} \tag{4.17}$$

$$\dot{X}_3 = \frac{X_2}{T_F} \tag{4.18}$$

The dot notations, $\dot{X}$ used, represents time derivatives of the state variables. The differential equations (4.16) to (4.18) are solved at each time step to give effectively by controlled field voltage, E_F.

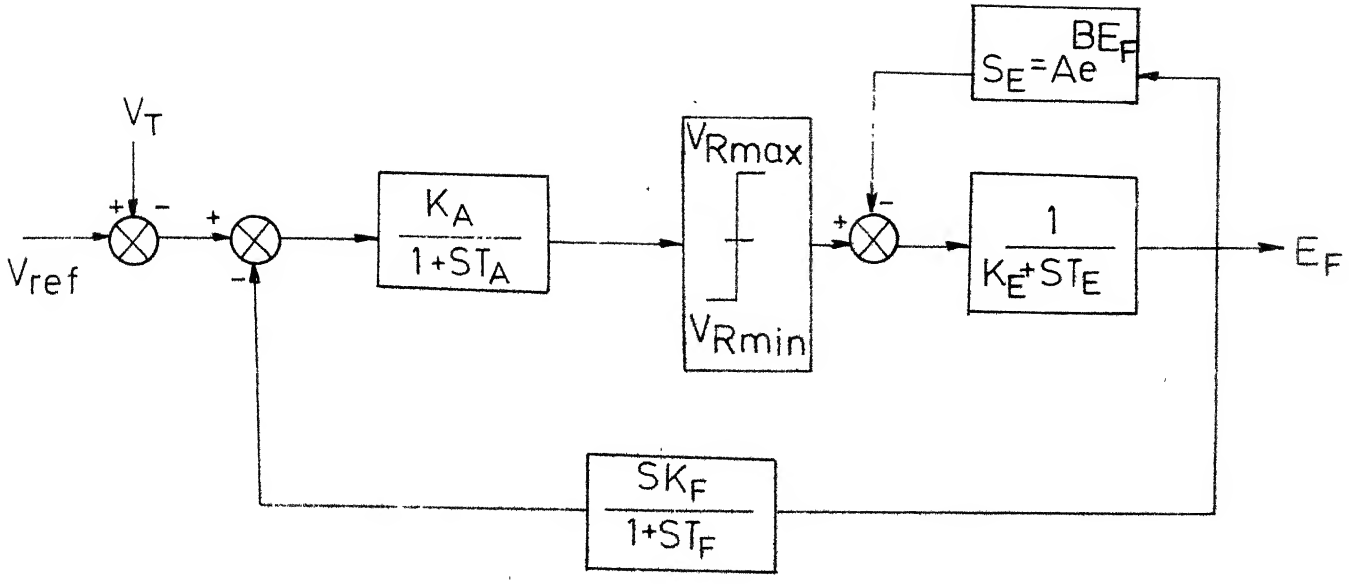

IEEE TYPE 1 ROTATING EXCITATION SYSTEM MODEL

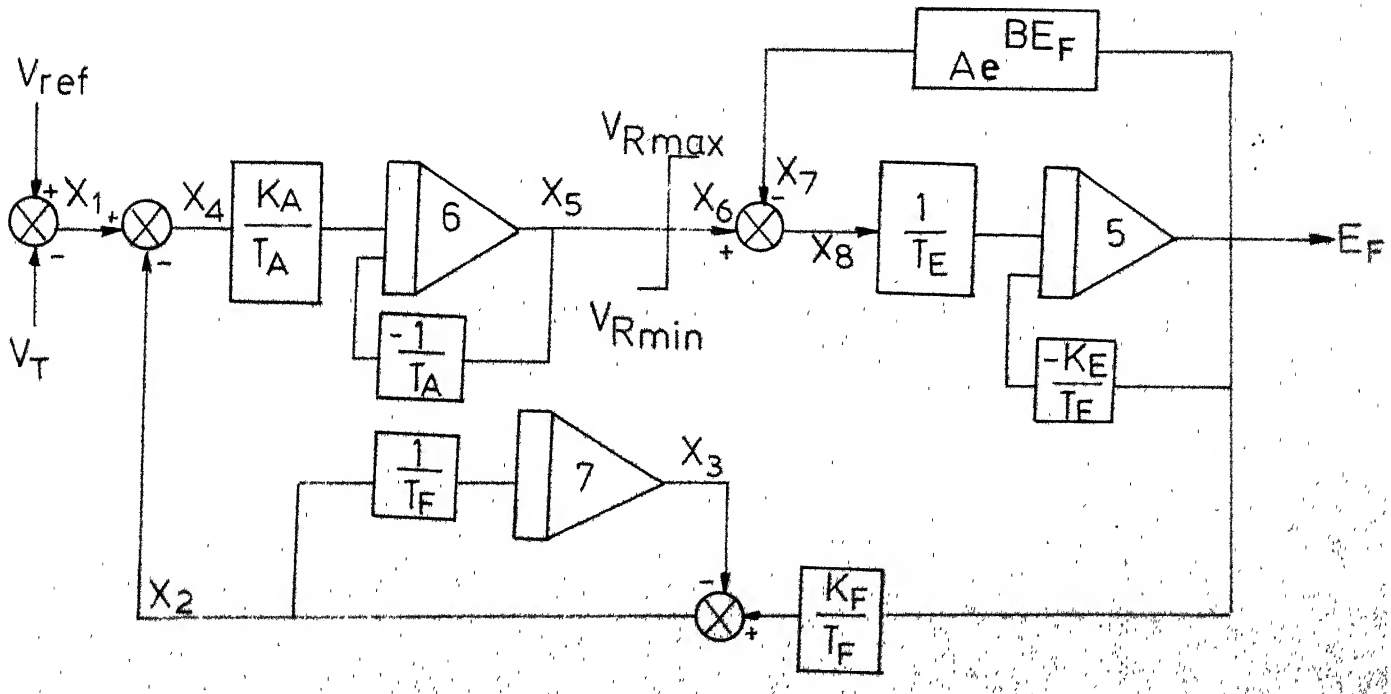

ANALOG DIAGRAM OF IEEE TYPE-1 ROTATING EXCITER

FIG. 4.3

CHAPTER 5

IMPLEMENTATION INCLUDING ELECTRICAL LOADING

5.1 General Discussion

In Chapter 3, we assumed that the total electrical demand of the loads plus network losses does not change even after the disturbance (generator trip-out). We wish to study this assumption in greater detail. Following generation trip-out, there will be changes in network losses due to redistribution of powers. Similarly there will be changes in voltages and frequency and this could also change load demand. Therefore, the total electrical power P_{eT} may change.

We shall now include representations of network, generator electrical parameters, excitation system and nature of loads. If loads were represented as constant P,Q type, obviously P_{eT} would also be a constant except for losses in the network. We shall represent loads by constant admittance which is given by

$$Y_p = \frac{P_p - jQ_p}{E_p^2}$$

where P_p and Q_p are the specified real and reactive powers for the pth load and E_p is the load bus voltage magnitude prior to the distirbance.

5.2 Calculation of Total Electrical Power Output P_{eT}

Let ϕ_j be the jth rotor angle measured with respect to system centre of inertia. Then the rotor angle θ_j measured with respect to synchronous reference frame can be expressed as

$$\theta_j = \phi_j + \theta_o \tag{5.1}$$

where θ_o = system centre of inertia or system centre of angle

ϕ_j = rotor angle of jth machine measured with respect to system centre of inertia

and θ_j = rotor angle of jth machine measured with respect to synchronous reference frame.

Now jth rotor equation of motion

$$M_j \dot{\omega}_j = (P_{mj} - P_{ej}) \tag{5.2}$$

can be rewritten as

$$M_j(\ddot{\phi}_j + \ddot{\theta}_o) = (P_{mj} - P_{ej}) \tag{5.3}$$

where $\ddot{\phi}_j + \ddot{\theta}_o = \ddot{\theta}_j = \dot{\omega}_j$

and $$\ddot{\theta}_o = \dot{\omega}_o = \frac{1}{M_T}(P_{mT} - P_{eT}) \tag{5.4}$$

Substituting equation (5.4) in (5.3), it becomes

$$P_{ej} = P_{mj} - \frac{M_j}{M_T}(P_{mT} - P_{eT}) - M_j \ddot{\phi}_j \tag{5.5}$$

Neglecting oscillatory power transfers from one rotor to another resulting from synchronizing oscillations leads

to the assumption that no generator rotor can be accelerating or decelerating relative to another during the time step of integration. It follows, therefore, that during this time, no rotor can be accelerating or decelerating relative to the system centre of inertia. This means that any change that takes place in ϕ_j during the time step of integration is assumed to occur at constant velocity. Hence $\ddot{\phi}_j$ in equation (5.5) can be set equal to zero. Therefore, generator j must be producing electrical power as given by the equation (5.6).

$$P_{ej} = P_{mj} - \frac{M_j}{M_T}(P_{mT} - P_{eT}) \qquad (5.6)$$

The system equations of motion are given below.

$$\frac{d\,\omega_o}{dt} = \frac{1}{M_T}(P_{mT} - P_{eT}) \qquad (5.7)$$

$$\frac{d\,\theta_o}{dt} = (\omega_o - \omega_s) \qquad (5.8)$$

and $$\dot{P}_{mj} = F(P_{mj}, \omega_o) \quad \text{where } j = 1,2,\ldots,n \qquad (5.9)$$

At any instant of time, knownig P_{eT}, equations (5.7) to (5.9) can be integrated forward by one time step Δt. From this the new values of ω_o, θ_o and P_{mj} are known at $(t+\Delta t)$. Only P_{eT} need to be calculated at $(t + \Delta t)$ so as to take care of changes in network losses and load powers. At this stage an iterative procedure is adopted by using a power flow solution method to calculate new P_{eT} as described below.

From the initial load flow conditions obtained prior to disturbance, E_q, E_I and E'_q are calculated using equations (4.1) to (4.3) respectively. The initial field voltage E_F is set equal to E_I. The excitation system equations are written symbolically as

$$\dot{E}_F = F(E_F, |V_T|) \tag{5.10}$$

The equations (4.4) and (5.10) are integrated forward one time step for each generator and the new values of E_I calculated from equation (4.5) set up the necessary constraint over the magnitude of generator internal voltage E_q via equation (4.6) and this together with the generator power calculated from equation (5.6) are specified at all generator internal buses which are added to the network, except at the slack bus where angle and E_q are specified. These buses are treated as the voltage controlled buses.

The generator admittance, $1/(r_a+j\ X_q)$, becomes a branch of the network. The generator terminal buses are treated as load buses with P and Q specified as zero. The loads are represented as constant admittances by using the relation

$$Y_p = \frac{P_p - j\ Q_p}{E_p^2} \tag{5.11}$$

The diagonal elements of Y-matrix are modified accordingly by Y_p. All the necessary information is available to carry

out a power flow solution. Gauss-Seidel power flow solution method was used to compute P_{eT} in the power-frequency transient simulation program.

Let the slack generator bus power obtained from power flow solution be 'P_{slack}' which provides the power needed to balance total network input against loads plus losses and let the slack generator power calculated from equation (5.6) be 'P_{es}'. If P_{slack} differs from P_{es}, it indicates that the slack generator is not having the same acceleration as the other generators which is contrary to the dynamic energy balance simulation procedure. However, the power flow solution provides a new value of P_{eT} and this can be expressed as

$$P_{eT(new)} = \sum_{\substack{j=1 \\ j\neq s}}^{n} P_{ej(old)} + P_{slack} \qquad (5.12)$$

where s = Slack machine number.

The above equation can also be written as

$$P_{eT(new)} = P_{eT(old)} + (P_{slack} - P_{es}) \qquad (5.13)$$

From equations (5.6) and (5.13), it can be shown that

$$P_{ej(new)} = P_{ej(old)} + \frac{M_j}{M_T}(P_{slack} - P_{es}) \qquad (5.14)$$

where j = 1,2,...,n.

The equations (5.14) provide new generatorpowers which form the input to a new power flow solution. The iterative

procedure between equations (5.14) and power flow solution is continued until $(P_{slack} - P_{es}) \leq \varepsilon$ where ε is a specified tolerance. At this stage, the P_{eT} at $(t + \Delta t)$ is correctly computed. Since all the conditions at $(t + \Delta t)$ are known, the equations of motion of system centre of inertia can be integrated forward one time step.

5.3 Digital Simulation

Representation of network, generators and exciters complicates the problem. Initially the power-frequency transients were simulated on IEEE-14 bus problem. A single line diagram of the network is given in Fig. 5.2. The bus conditions prior to disturbance, line data, transformer data, voltage controlled bus data, generators, exciters, speed governors and turbines data are given in Appendix II. Later on the study is carried out on UPSEB planning network model for which the required data is given in Appendix I. The data for speed governors and turbines is given in Tables 2.1 and 2.2.

5.4 Step by Step Algorithm for Implementation on Digital Computer

Step - 1: Read bus data corresponding to predisturbance conditions and also data for lines, transformers, shunt loads, generators, speed governors and turbines, excitation systems. The generator inertia constant H, r_a, X_d, X'_d and X_q are converted to the common base chosen (200 MVA).

Step - 2: From the line, transformer and shunt load data, Y-matrix is constructed.

Step - 3: Generator internal buses are added to the network through the generator admittance $1/(r_a + j\ X_q)$ which becomes a branch to the network. These buses are treated as voltage controlled buses where voltage magnitude $|\ E_q\ |$ is specified by equation (4.1) and P is specified from initial bus power conditions.

Step - 4: Initial conditions of state variables of generators, X_G, exciters, X_e and speed governors and turbines, X_T, are calculated from equations (4.1) to (4.3), (4.7) to (4.9), and (2.1) to (2.6) (for thermal), (2.16) to (2.18) (for hydro) respectively.

Step - 5: From initial conditions P_{eT}, P_{mT} and θ_o are calculated by making use of equations (3.1), (3.2) and (1.1) respectively. Total moment of inertia of the system M_T is calculated by

$$\sum_{j=1}^{n} M_j$$

Initially, $P_{mj} = P_{ej}$, $j = 1,2,\ldots,n$.

Step - 6: Generator trip-out condition is simulated and this is done as shown below..

$$P_{mj} = 0.0$$

$$P_{ej} = 0.0$$

$$M_T = M_T - M_j$$

where j=Trip-out generator number.

Step - 7: Load flow is carried out to obtain voltages and P_{eT} immediately after the disturbance.

Step - 8: Time derivatives of state variables of excitation systems, $\dot{X}_e$, speed governors and turbines, $\dot{X}_T$ and generators, $\dot{X}_G$ are calculated by equations (4.10) to (4.18),(2.7) to (2.15) (for thermal), (2.20) to (2.29) (for hydro) and (4.4) respectively and also

$$\frac{d\,\omega_o}{dt} = \frac{1}{M_T}(P_{mT} - P_{eT}) \quad \text{and} \quad \frac{d\,\theta_o}{dt} = (\omega_o - \omega_s)$$

are formed.

Step - 9: The differential equations obtained from Step-8 are solved by Modified Euler's method of integration. At this stage, state variables at $(t + \Delta t)$ are obtained. Time T is advanced by one time step ΔT. Frequency $f = \omega_o/2\pi$ is calculated.

Step - 10: New values of $|E_q|$ are specified at all generator internal buses by the equation (4.6). The generator powers, P, calculated from equation (5.6), are also specified at these buses, except at the slack bus. The slack bus angle is specified.

Step - 11: Load flow is performed to obtain new voltages and slack bus power. Let it be called as 'P_{slack}'. Compute slack machine power 'P_{es}' from equation (5.6).

Step - 12: If $(P_{slack} - P_{es}) \leq \varepsilon$, where ε is the specified tolerance. P_{eT} is computed and enter at Step-9. Otherwise go to Step-13.

Step - 13: At the generator internal buses, power P_j is modified by

$$P_{ej(new)} = P_{ej(old)} + \frac{M_j}{M_T} (P_{slack} - P_{es}).$$

Step - 14: Steps 11 to 14 are repeated until $(P_{slack}-P_{es}) \leq \varepsilon$. At this stage all P_{ej}s at $(t + \Delta t)$ are calculated correctly and P_{eT} is computed.

Step - 15: Steps 8 to 15 are repeated until the simulation period is finished.

Step - 16: The frequency is plotted against time. **Interrelationships between various subroutines is shown in Fig.5.1.**

5.5 Computer Results for IEEE-14 Bus System:

General Information:

Number of buses = 14

Number of lines = 20

Number of voltage controlled buses = 4

Number of shunt loads = 1

Number of generators = 2

Normal operating frequency = 50.0 Hz

System base MVA chosen = 100.0 MVA

Total moment of inertia M_T on 100MVA base = 0.102.

Initial velocity of system centre of inertia = $_0$ = 314.0 rad/sec.

Initial system centre of angle θ_0 = 0.3063 radians

Integration time step used = 0.1 sec.

Generator at bus No.2 meeting a load demand of 40.0 MW out of 272.4 MW is tripped-out, i.e. about 15% generation is dropped.

The total spinning reserve available at the time of disturbance which is sufficient to overcome the generation loss = 52.35 MVA.

The total electrical power generated prior to disturbance = 2.724 p.u. ~~MW~~.

The total mechanical power output prior to disturbance = 2.732 ~~MW~~. p.u.

The simulation results for loss of generation on IEEE-14 bus system are given in Table 5.1.

It is observed from the results given in Table 5.1, that the pre-disturbance ($t = 0^-$) electrical power P_{eT} is 2.724 p.u. ~~MW~~ and immediately after the disturbance ($t = 0^+$) is 2.733 p.u. ~~MW~~. The change in P_{eT} is therefore 0.34% compared to a 15% loss of generation. In 1972 Berg[6] reported actual field tests on a Norweign system. The total installed generating capacity of the system exceeded 2000 MW and amounts of generation loss ranged from 3% to 27% of the system load. The spinning reserve was adequate to compensate for generation loss. The very interesting conclusions were that a loss of generation of only a few percent had very little effect on the system voltage and frequency. For as great a loss as 27%, the voltage drop was less than 2 percent for the HV network, indicating that the total drop in electrical load is very small. This

is confirmed in the above IEEE-14 bus study carried out in time steps of 0.1 seconds upto 5.6 seconds. The reason for carrying out the study upto 5.6 seconds only was that in simulation program a not very efficient Gauss-Seidel load flow computer program had to be used repeatedly. It took 26 minutes of computer time in IBM 7044 to simulate only 5.6 seconds of transient. The graph is shown in Fig. 5.3. Such a large amount of computing time may be attributed to possible inefficient program besides the Gauss-Seidel load flow program. At this stage we wish to observe that it may be adequate to treat the electrical loading as constant at the pre-disturbance level. This observation is further substantiated when we take up the UP State planning model next.

5.6 Computer Results for UPSEB Planning Model Network

General Information:

Number of buses	= 96
Number of lines	= 136
Number of voltage controlled busses	= 27
Number of shunt loads	= 44
Number of generators	= 20
Normal operating frequency	= 50.0 Hz
System base MVA chosen	= 200.0
Total moment of inertia on 200 MVA base	= 0.602
Initial velocity of system centre of inertia	= 314.0 rad/sec.

Initial angle of system centre of inertia = θ_o = 0.2102 rad.

Integration time step used = 0.1

Slack bus number = 94.

Generator at Anpara power station having a capacity of 528 MVA meeting a load demand of 400 MW out of 5556.87 MW was tripped-out, i.e. about 7.2% generation was dropped.

The total spinning reserve available at the time of disturbance = 560 MVA which is sufficient to overcome the loss of generation.

The total electrical power generated prior to disturbance = 27.784 p.u. ~~MW~~.

The total electrical power output immediately after the disturbance = 27.912 p.u. MW.

The change in P_{eT} after the disturbance = 0.1287 p.u. ~~MW~~

∴Change in P_{eT} after the disturbance = 0.463%

Total mechanical power P_{mT} prior to disturbance = 27.841 p.u. ~~MW~~

Total mechanical power P_{mT} after the disturbance = 25.84 p.u. ~~MW~~

At 0.1 seconds after the disturbance, the system conditions are:

Angle of system centre of inertia θ_o = 0.2102 rad.

Velocity of system centre of inertia, ω_o = 313.808 rad/sec.

The frequency, f of the system = 49.99 Hz

Total mechanical power output, P_{mT} = 25.839 p.u.~~MW~~

Total electrical power output, P_{eT} = 27.912 p.u.~~MW~~

The simulation was carried out for only two time steps because of large computing time. However, it demonstrates our contention that electrical loading can be treated as constant. In that case the results obtained in Chapter 3 (Part - d) are adequate.

Table 5.1: Simulation Result for Loss of Generation on IEEE-14 Bus System.

S. No.	Time in sec.	θ_o (rad.)	ω_o (rad./sec)	f (Hz)	P_{mT} (p.u.MW)	P_{eT} (p.U.MW)
	0^-	0.3063	314.000	50.00	2.7332	2.724
	0^+	0.3063	314.000	50.00	2.3332	2.733
1	0.1	0.3063	313.687	49.99	2.331	2.733
2	0.2	0.2591	313.214	49.92	2.331	2.733
3	0.3	0.1646	312.663	49.85	2.264	2.733
4	0.4	0.0149	312.156	49.76	2.302	2.733
5	0.5	-0.1854	311.583	49.68	2.245	2.733
6	0.6	-0.4430	311.014	49.59	2.249	2.733
7	0.7	-0.7576	310.417	49.59	2.226	2.733
8	0.8	-1.1318	309.847	49.40	2.248	2.733
9	0.9	-1.5630	309.243	49.31	2.220	2.733
10	1.0	-2.0546	308.690	49.22	2.263	2.733
11	2.0	-9.9095	303.765	48.41	2.409	2.733
12	3.0	-21.6670	301.244	47.96	2.650	2.733
13	4.0	-34.6996	301.439	47.96	2.818	2.733
14	5.0	-46.8816	302.659	48.15	2.844	2.733
15	5.6	-53.5840	303.453	48.27	2.847	2.733

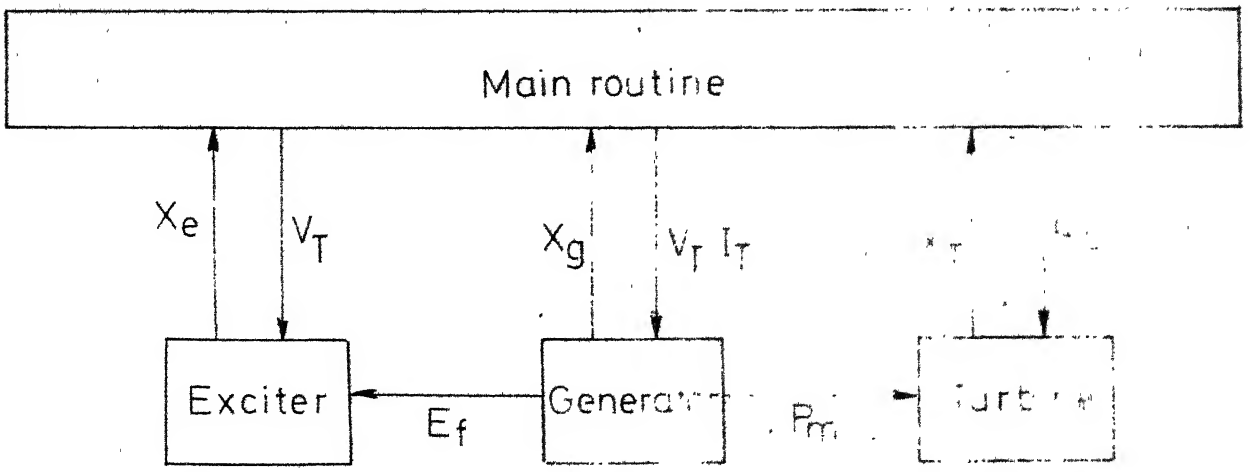

RELATIONSHIPS OF SUBROUTINES FOR INITIAL CONDITIONS

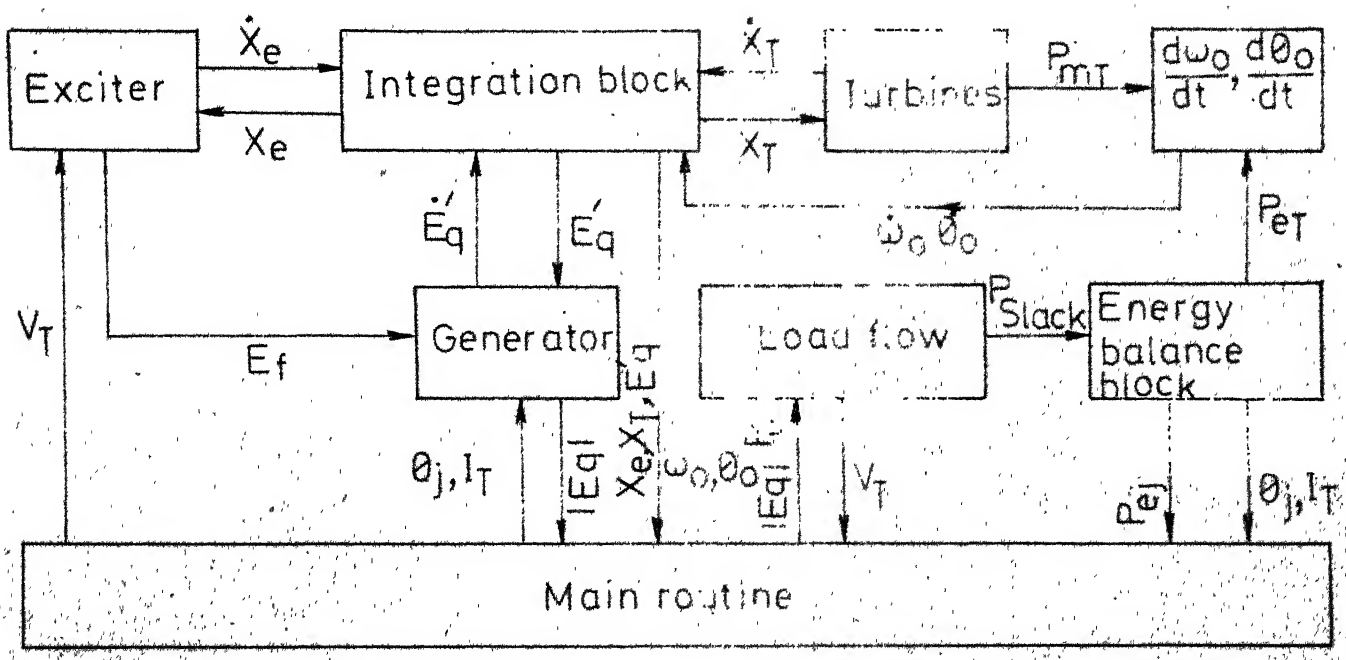

RELATIONSHIPS BETWEEN SUBROUTINES DURING STEP BY STEP SIMULATION

FIG 5.1

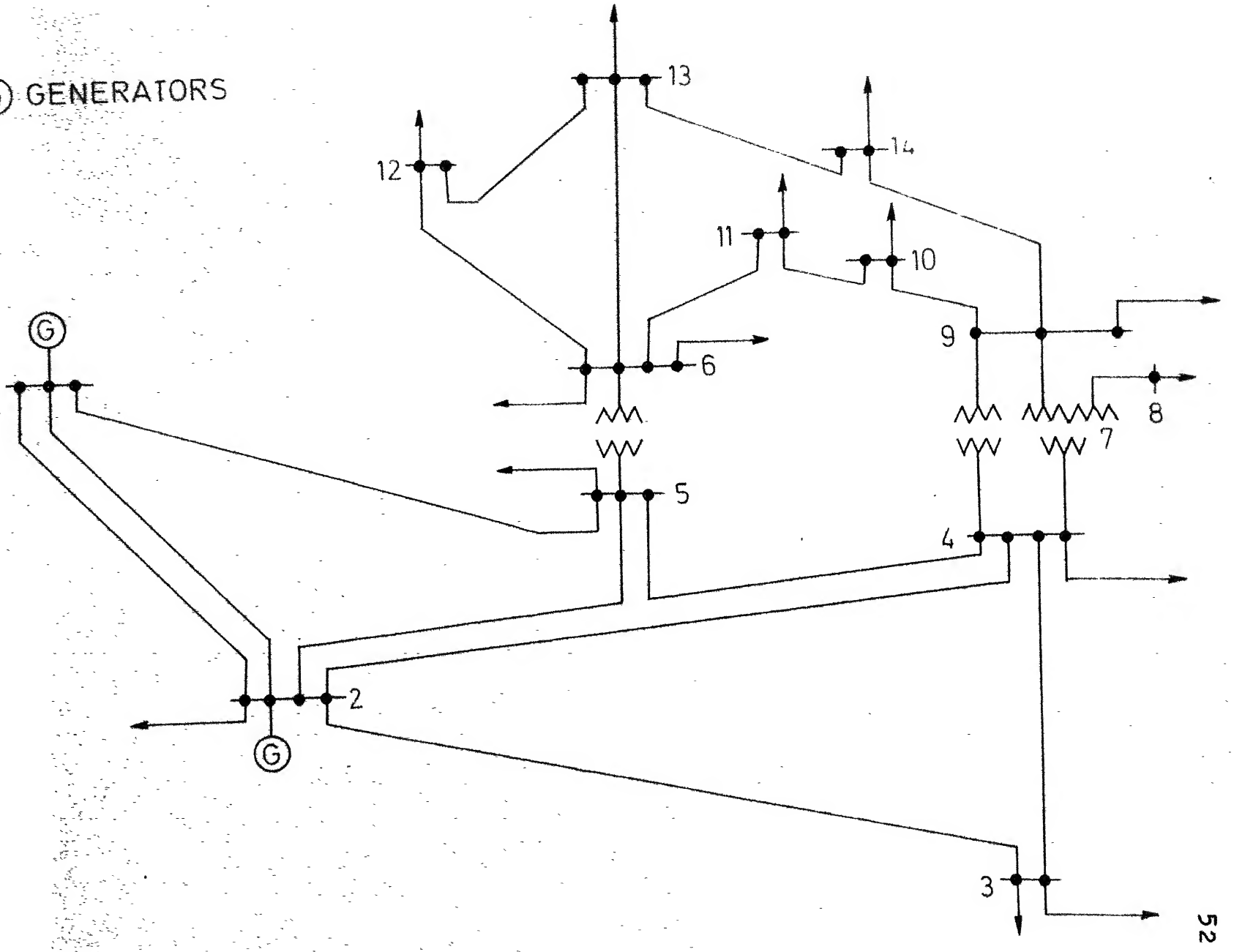

FIG. 5·2 SINGLE LINE DIAGRAM OF IEEE 14 BUS SYSTEM

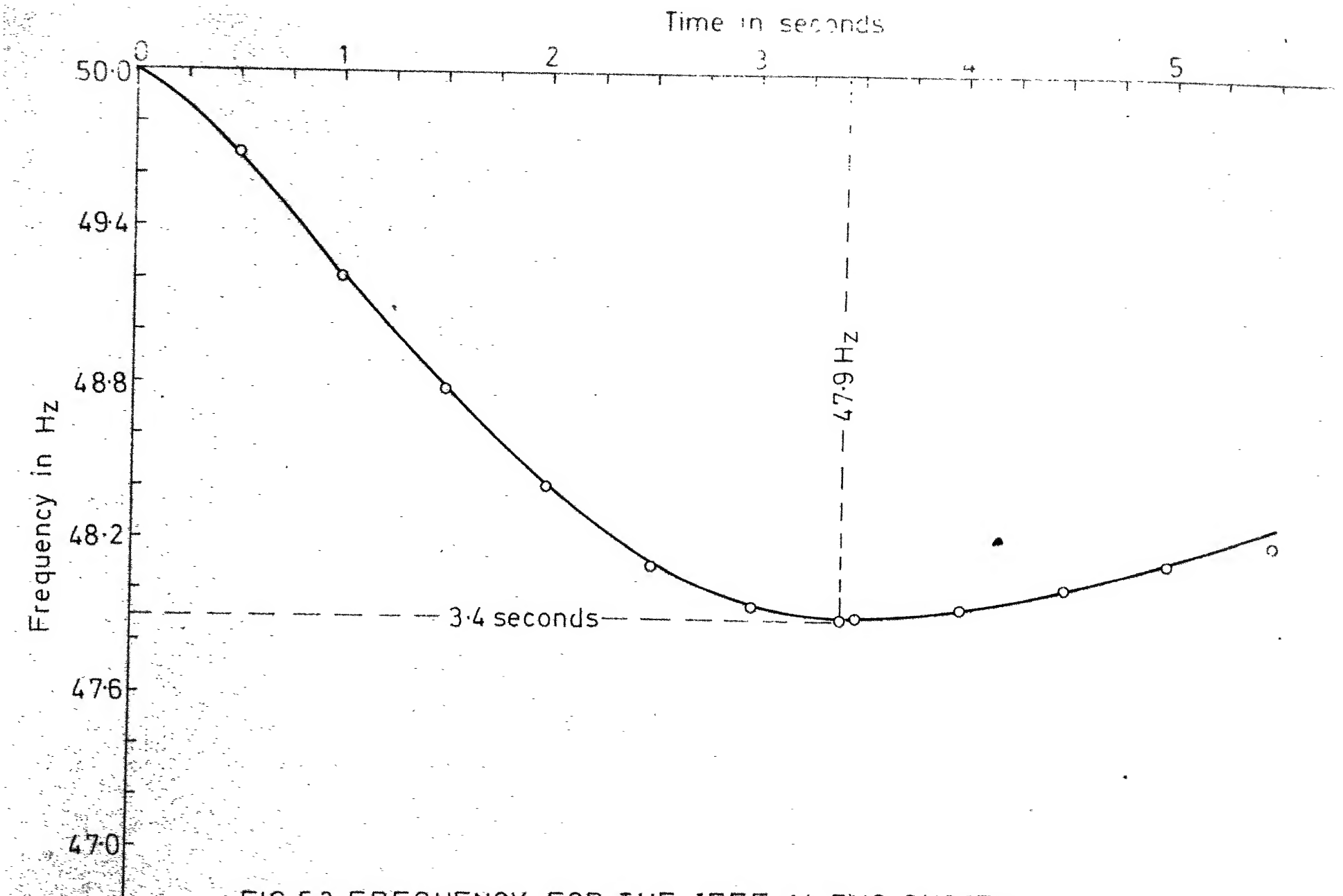

FIG. 5·3 FREQUENCY FOR THE IEEE-14 BUS SYSTEM

CHAPTER 6

OVERALL CONCLUSIONS AND SUGGESTIONS FOR FUTURE WORK

6.1 Overall Conclusions

The basic aim of this thesis was to simulate power-frequency transients following a loss of large block of generation and also to review Stanton's power-frequency transients simulation procedure using dynamic energy balance concepts. A realistic test problem had been chosen from one of the U.P. State electricity board planning model networks for the year 1984-85 to carry out the above studies.

At first to get the 'feel' for the problem, the frequency transients were simulated on the above system treating the entire system to have only thermal power generation and was represented by one equivalent machine of capacity equal to the total capacity of the system and by one equivalent hydro machine of capacity equal to the total capacity of the system respectively and also assuming that the total electrical loading to be same for the pre and post disturbance conditions. The spinning reserves were adequate to overcome the loss of generation. From the above studies, it was concluded that the system which is predominantly thermal can pick up the load much faster than an hydro system and also it was observed that the maximum frequency deviation from the normal value is much

less and settles to a steady state value faster than for an hydro system. This fact is because of smaller time constants involved in the thermal system and also due to the smaller moment of inertia compared to that of hydro systems.

In the next study the entire U.P.S.E.B. system was represented by one equivalent thermal machine with a capacity equal to all the thermal generation and one equivalent hydro machine equal to all the hydro generation. Since most of the thermal machines had similar time constants and the same was true for most of the hydro machines, it could be done without too much difficulty. Again the electrical loading was treated as constant. As expected, the results were in between those for a purely thermal and for a purely hydro system studied earlier. Later on the identity of all thermal and hydro stations was retained but the electrical loading was treated as constant. The results were not too different than the case of one equivalent thermal and one equivalent hydro machine. This was because of the similar time constants of various machines as already mentioned.

Finally, the simulation was performed taking into account the change in electrical loading. This required the representation of electrical network, generators, excitation systems and loads (by constant admittance).

Because of the complexity of the problem, first IEEE 14 bus system was studied. It was found that the electrical loading immediately after the disturbance was only about 0.5% different than the pre-fault electrical loading, and further the electrical loading stayed constant at the immediate post disturbance level through out the simulation period. Similar results were also obtained on UPSEB planning model. Field studies carried out by Berg on the actual Norwegian system also show similar results.

Thus it can be concluded that if the loads are treated either by constant P,Q or constant admittance representation, then the power-frequency transients can be simulated in a most economical way by considering only speed governor and turbine actions and treating the electrical loading constant. Fig. 6.1 shows the system frequency for three cases viz., 1) Treating entire UPSEB system by one equivalent thermal and one equivalent hydro machine, 2) Retaining the identity of all thermal and hydro stations and 3) The rotor angle of a generator close to the disturbance obtained from a transient stability program. Curves 1 and 2 are close together for reasons already given earlier. The trend of these two curves is similar to that obtained by transient stability study.

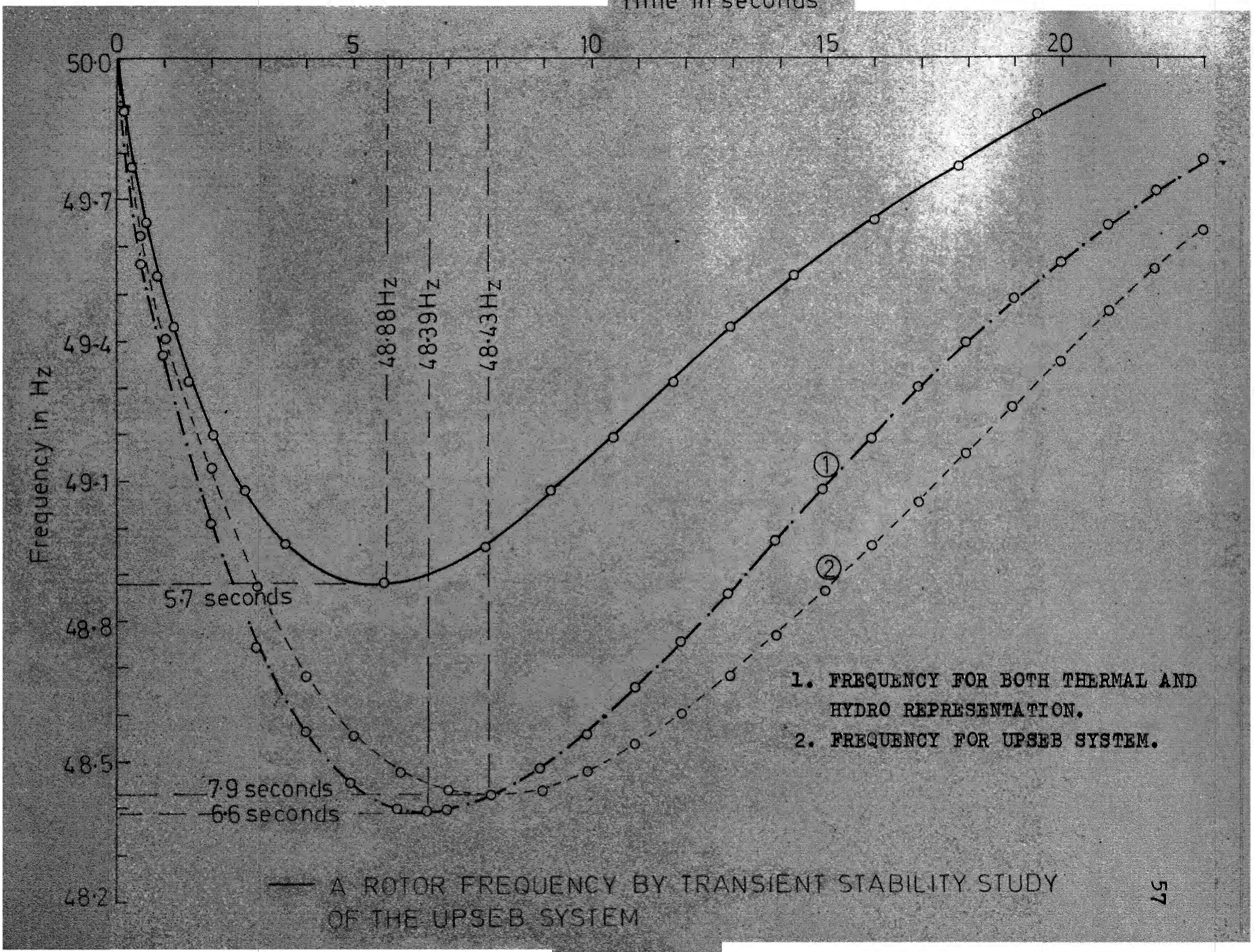

A ROTOR FREQUENCY BY TRANSIENT STABILITY STUDY OF THE UPSEB SYSTEM

FIG 5·1

6.2 Suggestions for Future Work

In this thesis, the loads have been represented by constant admittances. It would be desirable to consider other possible models like constant current, constant MVA and frequency dependence etc. More detailed models for large induction and synchronous motors which can take into account voltage and frequency changes should also be examined.

In the simulation method for power-frequency transients, the whole system was treated to have one equivalent velocity of system centre of inertia which may not be true. It may be necessary for large systems to divide into two or three equivalent areas. Unless this subdivision into different areas is performed, the power-frequency transients which we obtain may be quite different from the realistic values.

REFERENCES

1. K.Neil Stanton, "Dynamic Energy Balance Studies for Simulation of Power-Frequency Transients," Proc. Power Industry Computer Applications Conference, Boston, Mass, May 1971.

2. R. Podmore, "Power System Dynamic Simulation Program", Users Manual.

3. E.W. Kimbark, Synchronous Machines, Power System Stability, Vol.3, New York, Dover Publications Inc., 1968.

4. IEEE Committee Report, "Computer Representation of Excitation Systems", IEEE Trans. PAS, Vol. 87, pp. 1460-1464, June,1968.

5. Glenn W. Stagg and Ahmed, H. El-Abiad, Computer Methods in Power System Analysis, Tokyo, McGraw-Hill Kogakusha Ltd., 1968.

6. G.J.Berg, "System and Load Behaviour Following Loss of Generation, Experimental Results and Evaluation", Proc. IEE, Vol.119, No.10, October 1972.

7. V. Venikov, Transient Processes in Electrical Power Systems, Moscow, Mir Publishers, 1977.

8. A. Barzam, Automation in Electrical Power Systems, Moscow, Mir Publishers, 1977.

9. IEEE Press Press Publication, Stability of Large Electric Power Systems, New York, IEEE Press, 1974.

10. Olle1.Elgerd, Electric Energy Systems, Theory, An Introduction, New Delhi, Tata McGraw-Hill Publishing Company Ltd., 1971.

11. IEEE Committee report, "Dynamic Models for Steam and Hydro Turbines in Power System Studies", IEEE Trans.,PAS, Nov/Dec., 1973.

12. H.E. Lokay and V. Burtnyk, "Application of Underfrequency Relays for Automatic Load Shedding", IEEE Trans., PAS, January 1970.

APPENDIX I

UPSEB PLANNING MODEL NETWORK DATA

a) Bus Conditions Prior to Disturbance

Bus No.	GENERATION(MW)		LOAD POWER(MW)		Voltage Magnitude in p.u.	Phase angle in deg.
	P	Q	P	Q		
1	2	3	4	5	6	7
1	700.00	155.45	0.00	0.00	1.03	-1.528
2	0.00	0.00	0.00	0.00	1.06	-5.687
3	300.00	18°.07	0.00	0.00	1.02	-8.443
4	0.00	0.00	0.00	0.00	1.10	-10.946
5	736.00	460.00	0.00	0.00	1.04	2.934
6	0.00	0.00	0.00	0.00	1.07	-5.157
7	68.00	34.00	0.00	0.00	1.04	-9.123
8	0.00	0.00	40.00	25.00	1.09	-12.644
9	197.00	98.00	0.00	0.00	1.03	-10.117
10	0.00	0.00	230.00	128.30	1.09	-12.785
11	0.00	0.00	81.00	58.00	1.07	-14.358
12	0.00	0.00	0.00	0.00	1.03	-14.399
13	0.00	0.00	170.00	126.00	1.06	-17.431
14	0.00	0.00	0.00	0.00	0.97	-11.168
15	0.00	0.00	0.00	0.00	1.02	-15.573
16	0.00	0.00	154.00	134.00	1.02	-20.630
17	0.00	0.00	91.00	67.00	1.00	-21.606
18	0.00	101.42	0.00	0.00	1.00	-20.285
19	0.00	0.00	207.00	154.00	0.99	-23.731
20	0.00	0.00	0.00	0.00	0.97	-21.693

Contd..

1	2	3	4	5	6	7
21	0.00	0.00	72.00	52.00	1.00	-24.595
22	0.00	0.00	52.00	42.00	0.96	-20.441
23	0.00	0.00	86.00	63.00	1.01	-23.530
24	0.00	0.00	0.00	0.00	1.10	-11.592
25	0.00	0.00	87.00	64.00	1.06	-36.738
26	0.00	0.00	0.00	0.00	1.02	-11.546
27	0.00	0.00	142.20	100.00	1.02	-17.664
28	0.00	0.00	77.00	56.00	1.05	-20.671
29	190.00	120.00	0.00	0.00	0.95	-15.826
30	0.00	0.00	49.00	35.00	1.03	-17.824
31	0.00	0.00	0.00	0.00	1.02	-17.591
32	0.00	0.00	235.00	175.00	1.06	-20.503
33	95.00	39.89	0.00	0.00	1.05	-25.967
34	0.00	0.00	27.00	18.00	1.09	-27.757
35	0.00	0.00	0.00	0.00	1.01	-16.470
36	150.00	90.00	0.00	0.00	0.97	-14.050
37	0.00	0.00	77.00	57.00	1.02	-20.235
38	0.00	0.00	0.00	0.00	0.92	-24.184
39	0.00	0.00	227.00	170.00	1.02	-24.186
40	0.00	0.00	0.00	0.00	1.03	-13.219
41	0.00	0.00	0.00	0.00	1.04	-18.023
42	0.00	0.00	212.00	159.00	1.12	-22.058
43	0.00	0.00	0.00	0.00	1.00	-25.320
44	0.00	0.00	74.00	55.00	1.08	-28.925

Contd...

1	2	3	4	5	6	7
45	0.00	84.06	0.00	0.00	1.00	-30.522
46	0.00	0.00	78.00	65.00	1.03	-36.694
47	0.00	0.00	0.00	0.00	0.91	-41.889
48	0.00	0.00	153.00	135.00	0.98	-41.893
49	35.00	26.00	0.00	0.00	1.05	-37.435
50	0.00	0.00	13.00	11.40	1.00	-41.053
51	176.00	50.26	0.00	0.00	1.08	-31.856
52	0.00	0.00	8.00	5.00	1.05	-36.948
53	0.00	0.00	25.00	22.00	1.02	-39.506
54	0.00	28.43	45.00	39.00	1.00	-42.424
55	0.00	0.00	0.00	0.00	1.03	-33.411
56	0.00	0.00	0.00	0.00	0.98	-37.353
57	0.00	0.00	216.00	190.00	1.02	-40.825
58	0.00	0.00	139.00	104.00	1.03	-39.399
59	0.00	0.00	241.00	241.00	1.02	-30.842
60	400.00	248.00	0.00	0.00	0.99	-27.560
61	0.00	0.00	0.00	0.00	1.04	-33.236
62	191.00	114.00	0.00	0.00	0.96	-30.937
63	0.00	0.00	0.00	0.00	1.03	-34.291
64	50.00	39.31	0.00	0.00	1.05	-35.448
65	0.00	0.00	151.00	151.00	1.07	-37.811
66	0.00	53.35	0.00	0.00	1.00	-40.337
67	0.00	0.00	191.00	169.00	1.00	-44.161

Contd..

1	2	3	4	5	6	7
68	0.00	0.00	0.00	0.00	1.02	-34.749
69	0.00	0.00	175.00	153.00	1.05	-38.901
70	0.00	0.00	720.00	520.00	0.91	-30.837
71	0.00	335.94	32.00	34.00	1.00	-35.638
72	0.00	0.00	132.00	132.00	1.01	-39.787
73	0.00	0.00	0.00	0.00	0.97	-38.304
74	0.00	0.00	172.00	172.00	1.00	-40.865
75	0.00	0.00	69.00	69.00	1.02	-35.611
76	0.00	0.00	0.00	0.00	1.04	-33.422
77	0.00	0.00	102.00	102.00	1.07	-36.882
78	48.00	24.00	0.00	0.00	0.98	-33.657
79	0.00	0.00	0.00	0.00	1.06	-36.954
80	0.00	0.00	0.00	0.00	0.99	-36.398
81	0.00	0.00	75.00	58.00	1.06	-37.395
82	0.00	0.00	115.00	115.00	0.97	-39.655
83	152.00	40.09	0.00	0.00	1.05	-27.958
84	0.00	0.00	8.00	6.00	1.09	-31.759
85	272.00	80.00	0.00	0.00	0.98	-25.924
86	0.00	0.00	0.00	0.00	1.07	-30.318
87	89.00	45.00	0.00	0.00	0.99	-26.834
88	0.00	0.00	0.00	0.00	1.06	-31.652
89	191.00	95.00	0.00	0.00	1.00	-26.386
90	0.00	0.00	0.00	0.00	1.08	-30.449
91	0.00	0.00	0.00	0.00	0.96	-33.729

Contd..

1	2	3	4	5	6	7
92	0.00	0.00	53.00	53.00	1.07	-33.734
93	0.00	0.00	62.00	46.00	1.07	-35.580
94	1151.87	239.88	0.00	0.00	1.03	0.00
95	0.00	0.00	0.00	0.00	1.07	-5.394
96	365.00	156.19	0.00	0.00	1.03	-12.725

(b) Line Data (MVA Base = 200.0).

Line No.	From Bus	To Bus	Line Impedance (p.u.)		Half Line Charg.Admit. (p.u.)		Off Nom. Tr.Turns Ratio
1	2	3	4	5	6	7	8
1	1	2	0.00000	0.02380	0.0	0.00000	0.950
2	2	4	0.00000	0.06250	0.0	0.00000	0.925
3	2	6	0.00123	0.01248	0.0	0.04077	1.000
4	95	14	0.00817	0.08320	0.0	0.27180	1.000
5	2	26	0.00972	0.09900	0.0	0.32344	1.000
6	3	4	0.00000	0.03640	0.0	0.00000	0.900
7	4	8	0.00940	0.08303	0.0	0.00026	1.000
8	4	10	0.06552	0.35417	0.0	0.00425	1.000
9	4	12	0.01637	0.07823	0.0	0.06669	1.000
10	4	31	0.01976	0.09608	0.0	0.18158	1.000
11	4	24	0.01171	0.05943	0.0	0.01180	1.000
12	5	6	0.00000	0.04760	0.0	0.00000	0.900
13	6	35	0.01735	0.10506	0.0	0.57010	1.000
14	7	8	0.00000	0.22200	0.0	0.00000	0.925
15	8	10	0.03184	0.07578	0.0	0.00872	1.000
16	8	11	0.03184	0.07578	0.0	0.00872	1.000
17	9	10	0.00000	0.05700	0.0	0.00000	0.925
18	24	10	0.00000	0.10000	0.0	0.00000	1.000
19	10	11	0.05282	0.12571	0.0	0.01447	1.000
20	11	13	0.06706	0.15959	0.0	0.01837	1.000
21	12	13	0.00000	0.06860	0.0	0.00000	0.925

Contd..

1	2	3	4	5	6	7	8
22	12	15	0.03514	0.17829	0.0	0.03540	1.000
23	13	17	0.09150	0.21777	0.0	0.02507	1.000
24	14	15	0.00000	0.06250	0.0	0.00000	0.900
25	15	16	0.00000	0.10000	0.0	0.00000	0.925
26	15	18	0.03514	0.17828	0.0	0.03540	1.000
27	16	17	0.04158	0.09896	0.0	0.01139	1.000
28	17	19	0.09946	0.23671	0.0	0.02725	1.000
29	18	19	0.00000	0.06000	0.0	0.00000	0.975
30	18	20	0.02175	0.11037	0.0	0.02192	1.000
31	18	30	0.01332	0.06708	0.0	0.05448	1.000
32	19	21	0.12036	0.30234	0.0	0.00781	1.000
33	20	21	0.00000	0.20000	0.0	0.00000	0.925
34	21	23	0.12448	0.31345	0.0	0.00806	1.000
35	22	23	0.00000	0.20000	0.0	0.00000	0.925
36	22	27	0.02008	0.10189	0.0	0.02023	1.000
37	23	28	0.11190	0.27929	0.0	0.00722	1.000
38	26	40	0.00597	0.06019	0.0	0.19665	1.000
39	26	27	0.00000	0.06250	0.0	0.00000	0.950
40	27	28	0.00000	0.10000	0.0	0.00000	0.950
41	27	30	0.01165	0.05869	0.0	0.04766	1.000
42	28	32	0.20779	0.52192	0.0	0.01349	1.000
43	29	30	0.00000	0.03960	0.0	0.00000	0.900
44	31	32	0.00000	0.04980	0.0	0.00000	0.925
45	31	37	0.03459	0.16537	0.0	0.14097	1.000
46	33	34	0.00000	0.07920	0.0	0.00000	0.950

Contd..

1	2	3	4	5	6	7	8
47	34	59	0.04184	0.21225	0.0	0.16860	1.000
48	35	37	0.00000	0.06250	0.0	0.00000	0.975
49	35	70	0.00796	0.04865	0.0	1.05948	1.000
50	35	2	0.01592	0.09734	0.0	0.53001	1.000
51	36	37	0.00000	0.15840	0.0	0.00000	0.900
52	37	39	0.00000	0.06660	0.0	0.00000	0.950
53	37	59	0.02594	0.12398	0.0	0.10569	1.000
54	38	39	0.00000	0.27500	0.0	0.00000	0.900
55	40	41	0.00000	0.06250	0.0	0.00000	0.950
56	41	37	0.01016	0.04854	0.0	0.04138	1.000
57	41	42	0.00000	0.06440	0.0	0.00000	0.900
58	41	43	0.02677	0.13584	0.0	0.02698	1.000
59	42	44	0.16080	0.40390	0.0	0.01044	1.000
60	43	44	0.00000	0.20000	0.0	0.00000	0.900
61	43	45	0.02845	0.14433	0.0	0.02866	1.000
62	44	46	0.17241	0.43305	0.0	0.01119	1.000
63	45	46	0.00000	0.20000	0.0	0.00000	0.925
64	46	48	0.07643	0.18188	0.0	0.02094	1.000
65	47	48	0.00000	0.20000	0.0	0.00000	0.925
66	48	50	0.07886	0.18768	0.0	0.02160	1.000
67	48	54	0.16848	0.42417	0.0	0.01091	1.000
68	48	57	0.08317	0.19793	0.0	0.02278	1.000
69	49	50	0.00000	0.38000	0.0	0.00000	1.000
70	51	52	0.00000	0.11400	0.0	0.00000	1.000

Contd...

1	2	3	4	5	6	7	8
71	52	53	0.04680	0.11760	0.0	0.01215	1.000
72	52	58	0.05339	0.12705	0.0	0.01462	1.000
73	53	54	0.09360	0.23510	0.0	0.00607	1.000
74	53	57	0.09921	0.24921	0.0	0.00604	1.000
75	56	55	0.02295	0.23410	0.0	0.06965	1.000
76	56	61	0.02577	0.12964	0.0	0.02641	1.000
77	57	58	0.06359	0.15135	0.0	0.01742	1.000
78	57	72	0.23980	0.60373	0.0	0.01553	1.000
79	58	79	0.08143	0.20497	0.0	0.02108	1.000
80	58	81	0.08148	0.19392	0.0	0.02232	1.000
81	59	63	0.02133	0.10194	0.0	0.08690	1.000
82	60	61	0.00000	0.05690	0.0	0.00000	0.900
83	61	63	0.01165	0.05863	0.0	0.01194	1.000
84	61	68	0.00666	0.03183	0.0	0.02714	1.000
85	62	63	0.00000	0.06740	0.0	0.00000	0.900
86	63	65	0.00000	0.07760	0.0	0.00000	0.950
87	63	66	0.03179	0.16131	0.0	0.03203	1.000
88	63	68	0.00749	0.03581	0.0	0.03053	1.000
89	64	65	0.00000	0.19500	0.0	0.00000	0.950
90	65	67	0.18210	0.45750	0.0	0.01182	1.000
91	65	69	0.08424	0.21159	0.0	0.00547	1.000
92	66	67	0.00000	0.10000	0.0	0.00000	0.975
93	68	69	0.00000	0.09700	0.0	0.00000	0.950
94	68	71	0.00999	0.04775	0.0	0.04070	1.000

Contd..

1	2	3	4	5	6	7	8
95	69	72	0.11232	0.28212	0.0	0.00729	1.000
96	70	71	0.00000	0.06250	0.0	0.00000	1.050
97	71	55	0.02436	0.24760	0.0	0.07380	1.000
98	71	73	0.01466	0.07437	0.0	0.01477	1.000
99	71	72	0.00000	0.07800	0.0	0.00000	0.975
100	71	75	0.02884	0.14557	0.0	0.02942	1.000
101	72	74	0.02274	0.05713	0.0	0.00590	1.000
102	73	74	0.00000	0.09320	0.0	0.00000	0.950
103	75	76	0.02314	0.11642	0.0	0.02371	1.000
104	76	77	0.00000	0.10180	0.0	0.00000	0.950
105	76	86	0.01669	0.08432	0.0	0.06784	1.000
106	76	90	0.04016	0.20376	0.0	0.04046	1.000
107	77	81	0.02875	0.06843	0.0	0.00787	1.000
108	78	79	0.00000	0.27500	0.0	0.00000	0.900
109	79	81	0.06552	0.16495	0.0	0.00424	1.000
110	79	25	0.01892	0.04612	0.0	0.00121	1.000
111	80	81	0.00000	0.10000	0.0	0.00000	0.925
112	80	55	0.01864	0.09380	0.0	0.01910	1.000
113	80	82	0.02677	0.13584	0.0	0.02697	1.000
114	81	25	0.02434	0.06113	0.0	0.00632	1.000
115	82	73	0.02677	0.13584	0.0	0.02697	1.000
116	83	84	0.00000	0.10480	0.0	0.00000	0.950
117	84	86	0.02434	0.26126	0.0	0.00157	1.000
118	84	92	0.01965	0.04997	0.0	0.02036	1.000

Contd..

1	2	3	4	5	6	7	8
119	85	86	0.00000	0.06580	0.0	0.00000	0.900
120	86	55	0.02664	0.13410	0.0	0.02727	1.000
121	87	88	0.00000	0.21930	0.0	0.00000	0.900
122	88	55	0.01673	0.08490	0.0	0.06744	1.000
123	89	90	0.00000	0.08900	0.0	0.00000	0.900
124	90	55	0.02008	0.10188	0.0	0.08092	1.000
125	91	92	0.00000	0.20000	0.0	0.00000	0.900
126	92	93	0.02465	0.05960	0.0	0.01382	1.000
127	55	93	0.00000	0.10160	0.0	0.00000	0.925
128	93	25	0.01435	0.03613	0.0	0.00836	1.000
129	56	57	0.00000	0.06850	0.0	0.00000	0.925
130	96	41	0.00000	0.05690	0.0	0.00000	0.950
131	94	95	0.00000	0.01890	0.0	0.00000	0.950
132	95	6	0.00081	0.00832	0.0	0.02700	1.000
133	95	2	0.00081	0.00832	0.0	0.02700	1.000
134	95	26	0.00972	0.09900	0.0	0.32344	1.000
135	95	35	0.01726	0.10500	0.0	0.57010	1.000
136	95	40	0.01365	0.14890	0.0	0.49000	1.000

c) Voltage Controlled Bus Data

S.No.	Bus No.	Q-Minimum MVAR	Q-Maximum MVAR	Scheduled bus voltage(p.u.)
1	2	3	4	5
1	3	0.0	214.0	1.02
2	5	0.0	460.0	1.05
3	7	0.0	34.0	1.05
4	9	0.0	98.0	1.05
5	29	0.0	120.0	1.05
6	33	0.0	57.0	1.05
7	36	0.0	90.0	1.05
8	38	0.0	100.0	1.05
9	49	0.0	26.0	1.075
10	51	0.0	88.0	1.075
11	60	0.0	248.0	1.05
12	62	0.0	114.0	1.05
13	64	0.0	40.0	1.05
14	78	0.0	24.0	1.05
15	83	0.0	76.0	1.05
16	85	0.0	80.0	1.05
17	87	0.0	45.0	1.05
18	89	0.0	95.0	1.05
19	18	0.0	500.0	1.0
20	45	0.0	500.0	1.0

Contd..

1	2	3	4	5
21	54	0.0	500.0	1.0
22	66	0.0	500.0	1.0
23	71	0.0	500.0	1.0
24	1	0.0	445.0	1.025
25	96	0.0	200.0	1.025
26	59	0.0	500.0	1.0
27	81	0.0	500.0	1.0

d) Shunt Load Data

S.No.	Bus No.	Shunt Load Admittance(p.u.)	
1	2	3	4
1	11	0.0	0.065
2	13	0.0	0.020
3	16	0.0	0.010
4	17	0.0	0.085
5	19	0.0	0.160
6	21	0.0	0.035
7	23	0.0	0.080
8	27	0.0	0.120
9	28	0.0	0.070
10	32	0.0	0.030
11	39	0.0	0.070
12	42	0.0	0.125
13	44	0.0	0.100
14	46	0.0	0.180
15	48	0.0	0.350
16	54	0.0	0.080
17	57	0.0	0.500
18	58	0.0	0.230
19	59	0.0	0.800
20	65	0.0	0.450
21	67	0.0	0.520
22	69	0.0	0.450

Contd..

1	2	3	4
23	71	0.0	0.250
24	72	0.0	0.500
25	74	0.0	0.520
26	75	0.0	0.280
27	77	0.0	0.270
28	81	0.0	0.120
29	82	0.0	0.520
30	92	0.0	0.030
31	93	0.0	0.020
32	25	0.0	0.050
33	2	0.0	-0.750
34	6	0.0	-0.250
35	14	0.0	-0.250
36	26	0.0	-0.500
37	35	0.0	-1.000
38	40	0.0	0.000
39	70	0.0	-0.500
40	95	0.0	-0.500
41	18	0.0	0.500
42	45	0.0	0.420
43	66	0.0	0.265
44	70	0.0	1.670

e) Generator Parameters

S.No.	Base MVA	H (seconds)	r_a	X_d	X'_d	X_q
1	940.0	2.20	0.00179	2.117	0.287	2.117
2	422.5	2.71	0.00138	1.840	0.242	1.780
*3	940.0	2.20	0.00179	0.287	0.287	0.287
4	110.0	3.50	0.00600	0.901	0.290	0.559
5	335.0	3.99	0.00500	0.950	0.335	0.600
6	275.0	2.00	0.00100	2.170	0.300	2.050
7	139.0	2.00	0.00100	2.170	0.300	2.050
8	217.5	2.20	0.00270	1.700	0.290	1.650
* 9	51.75	4.00	0.00500	0.280	0.280	0.280
*10	220.0	4.94	0.00670	0.250	0.250	0.250
*11	528.0	1.91	0.00100	0.280	0.280	0.280
*12	340.0	2.53	0.00270	0.212	0.212	0.212
*13	75.0	3.50	0.00500	0.250	0.250	0.250
14	160.0	4.55	0.00300	0.950	0.300	0.600
15	211.0	3.40	0.00500	0.950	0.310	0.600
16	376.0	3.79	0.00314	0.950	0.280	0.600
17	103.5	2.85	0.00279	0.958	0.268	0.600
18	223.0	3.00	0.00300	0.950	0.300	0.600
‡19	1420.0	2.10	0.00230	2.350	0.280	2.150
20	490.0	2.20	0.00230	2.120	0.287	2.120

*These are treated as constant excitation machines.

‡Slack Generator.

f) Excitation System Data

S. No.	Gen. No.	K_A	K_E	K_F	T_A	T_E	T_F	V_{Rmin}	V_{Rmax}
1	1	250	1.0	0.12	0.04	0.20	3.5	-5	5
2	2	200	1.0	0.175	0.04	1.0	3.5	-5	5
3	4	200	1.0	0.12	0.50	0.7	2.0	-4	4
4	5	200	1.0	0.12	0.50	0.7	2.0	-4	4
5	6	200	1.0	0.10	0.02	1.38	3.0	-5	5
6	7	200	1.0	0.10	0.02	1.38	3.0	-5	5
7	8	200	1.0	0.10	0.02	1.38	3.0	-5	5
8	14	200	1.0	0.12	0.50	0.70	2.0	-4	4
9	15	200	1.0	0.12	0.50	0 70	2.0	-4	4
10	16	200	1.0	0.12	0.50	0.70	2.0	-4	4
11	17	200	1.0	0.12	0.50	0.70	2.0	-4	4
12	18	200	1.0	0.12	0.50	0.70	2.0	-4	4
13	19	600	1.0	0.00	10.72	0.47	100.0	2.1	11.5
14	20	250	1.0	0.12	0.04	0.20	3.5	-5	5

APPENDIX II

IEEE-14 BUS SYSTEM DATA

a) Bus Conditions Prior to Disturbance

Bus No.	Generation(MW) P	Q	Load Power (MW) P	Q	Voltage Magnitude in p.u.	Phase angle in degrees
1	232.4	-16.9	0.0	0.0	1.06	0.0
2	40.0	42.4	21.7	12.7	1.05	-4.98
3	0.0	23.4	94.2	19.0	1.01	-12.72
4	0.0	0.0	47.8	-3.9	1.02	-10.33
5	0.0	0.0	7.6	1.6	1.02	-8.78
6	0.0	12.2	11.2	7.5	1.07	-14.22
7	0.0	0.0	0.0	0.0	1.06	-13.37
8	0.0	17.8	0.0	0.0	1.09	-13.36
9	0.0	0.0	29.5	16.6	1.06	-14.94
10	0.0	0.0	9.0	5.8	1.05	-15.14
11	0.0	0.0	3.5	1.8	1.06	-14.79
12	0.0	0.0	6.1	1.6	1.06	-15.07
13	0.0	0.0	13.5	5.8	1.05	-15.16
14	0.0	0.0	14.9	5.0	1.04	-16.04

b) Line Data (Base MVA = 100.0)

Line No.	From Bus	To Bus	Line Impedance (p.u.)		Half Line Charg.Admit. (p.u.)		Off Nom. Tr.Turns Ratio
1	1	2	0.01938	0.05917	0.0	0.0264	1.000
2	1	5	0.05403	0.22304	0.0	0.0264	1.000
3	2	3	0.04699	0.19797	0.0	0.0219	1.000
4	2	4	0.05811	0.17632	0.0	0.1879	1.000
5	2	5	0.05695	0.17388	0.0	0.0170	1.000
6	3	4	0.06701	0.17103	0.0	0.1730	1.000
7	4	5	0.01335	0.04211	0.0	0.0064	1.000
8	4	7	0.00000	0.02091	0.0	0.0000	0.978
9	4	9	0.00000	0.55618	0.0	0.0000	0.969
10	5	6	0.00000	0.25202	0.0	0.0000	0.932
11	6	11	0.09480	0.19892	0.0	0.0000	1.000
12	6	12	0.12291	0.25581	0.0	0.0000	1.000
13	6	13	0.06615	0.13027	0.0	0.0000	1.000
14	7	8	0.00000	0.17615	0.0	0.0000	1.000
15	7	9	0.00000	0.11001	0.0	0.0000	1.000
16	9	10	0.03181	0.08450	0.0	0.0000	1.000
17	9	14	0.12711	0.27038	0.0	0.0000	1.000
18	10	11	0.08205	0.19207	0.0	0.0000	1.000
19	12	13	0.22092	0.19988	0.0	0.0000	1.000
20	13	14	0.17093	0.34802	0.0	0.0000	1.000

c) Voltage Controlled Bus Data

S.No.	Bus. No.	Q-Minimum MVAR	Q-Maximum MVAR	Scheduled bus voltage (p.u.)
1	2	-40.0	50.0	1.045
2	3	0.0	40.0	1.010
3	6	-6.0	24.0	1.070
4	8	-6.0	24.0	1.090

d) Shunt Load Data

S.No.	Bus No.	Shunt Load Admittance (p.u.)	
1	9	0.0	0.19

e) Generator Parameters

S.No.	Base MVA	H (seconds)	r_a	xX_d	X'_d	ZX_q
1	335.0	3.99	0.005	0.95	0.335	0.60
2	75.0	3.50	0.005	0.25	0.250	0.25

f) Excitation System Data

S. No.	Gen. No.	K_A	K_E	K_F	T_A	T_E	T_F	V_{Rmin}	V_{Rmax}
1	1	200	1.0	0.12	0.5	0.7	2.0	-4	4
2	2	200	1.0	0.12	0.5	0.7	2.0	-4	4

g) Turbine Parameters

Machine No.1:

P_{base} = 335.0

T_W = 1.0

T_S = 0.015

T_R = 5.0

= 0.04

= 0.30

$\dot{g}_{min}$ = -0.2

$\dot{g}_{max}$ = 0.1

g_{min} = 0.0

g_{max} = 0.85

Machine No.2:

P_{base} = 75.0

T_{HP} = 0.2

T_{IP} = 4.0

T_{LP} = 1000.0

F_{HP} = 0.62

F_{IP} = 0.38

F_{LP} = 0.0

R = 0.04

T_S = 0.425

$\dot{g}_{min}$ = -1.18

$\dot{g}_{max}$ = 0.59

g_{min} = 0.0

g_{max} = 0.74